REVIEW

The Use and Misuse of Conditional Symmetric Instability

DAVID M. SCHULTZ
NOAA/National Severe Storms Laboratory, Norman, Oklahoma

PHILIP N. SCHUMACHER
NOAA/National Weather Service, Sioux Falls, South Dakota

(Manuscript received 15 June 1998, in final form 14 December 1998)

ABSTRACT

A commonly employed explanation for single- and multiple-banded clouds and precipitation in the extratropics is slantwise convection due to the release of moist symmetric instability (MSI), of which one type is conditional symmetric instability (CSI). This article presents a review of CSI with the intent of synthesizing the results from previous observational, theoretical, and modeling studies. This review contends that CSI as a diagnostic tool to assess slantwise convection has been, and continues to be, misused and overused. Drawing parallels to an ingredients-based methodology for forecasting deep, moist convection that requires the simultaneous presence of instability, moisture, and lift, some of the misapplications of CSI can be clarified. Many of these pitfalls have been noted by earlier authors, but are, nevertheless, often understated, misinterpreted, or neglected by later researchers and forecasters. Topics include the evaluation of the potential for slantwise convection, the relationship between frontogenesis and MSI, the coexistence of moist gravitational instability and MSI, the nature of banding associated with slantwise convection, and the diagnosis of slantwise convection using mesoscale numerical models. The review concludes with suggested directions for future observational, theoretical, and diagnostic investigation.

1. Introduction

Single- and multiple-banded [hereafter, *banded* (Huschke 1959, p. 57)] clouds and precipitation are commonly observed in association with frontal zones in extratropical cyclones (e.g., Hobbs 1978; Houze 1993, section 11.4). Proposed explanations for these bands (e.g., Parsons and Hobbs 1983; Emanuel 1990) include frontogenesis, boundary layer instabilities, ducted gravity waves, Kelvin–Helmholtz instability, and moist slantwise convection due to the release of conditional symmetric instability (CSI; symbols and acronyms appearing in this article are listed in the appendix). A precise definition for CSI, a type of moist symmetric instability (MSI), is given in section 3b. Indeed, some observational studies over extended periods of time show the presence of MSI in association with banded precipitating baroclinic systems to be rather common (e.g., Bennetts and Sharp 1982; Seltzer et al. 1985; Byrd 1989; Reuter and Yau 1990, 1993; Reuter and Aktary 1993, 1995).

Although we do not deny the likely existence of slantwise convection or the possible involvement of MSI in some precipitating systems in the atmosphere, it is our contention that CSI is frequently misused and overused as a diagnostic tool, a point also noted by Wiesmueller and Zubrick (1998, p. 86). We believe the following four reasons are responsible, in part, for the present situation. 1) The theory of CSI has certain limitations and caveats that are discussed by earlier authors, but often are understated, misinterpreted, or neglected by later researchers and forecasters who rely on CSI as an explanation for banded precipitation. As the concept of CSI has grown in popularity and usage over time (Fig. 1), these qualifications are often omitted as second-generation references are cited at an increasing rate, instead of the older, but perhaps more correct, references. 2) With the advent of satellite imagery and Doppler radar with higher resolution than was available previously, banded cloud and precipitation features are observed frequently and demand explanation. These bands possess many of the characteristics expected from CSI theory (Emanuel 1983c, p. 233) and they tend to be present in regions where the criteria for CSI are satisfied. Hence, CSI typically is concluded to have played a role in their formation, at the expense of other, perhaps more plausible, mechanisms. 3) Due to the availability of gridded

Corresponding author address: Dr. David M. Schultz, NOAA/National Severe Storms Laboratory, 1313 Halley Circle, Norman, OK 73069.
E-mail: schultz@nssl.noaa.gov

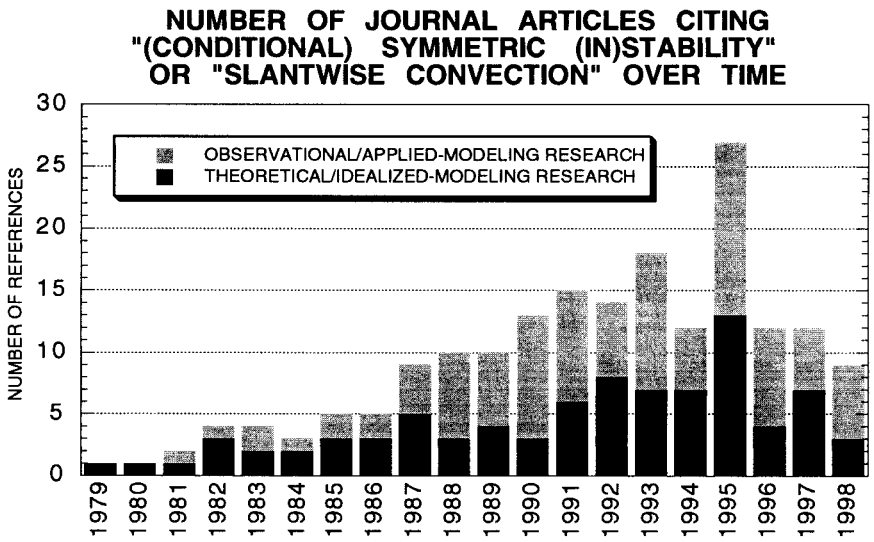

FIG. 1. Number of formal publications that cite atmospheric ''(conditional) symmetric (in)stability'' or ''slantwise convection'' as a function of time. Articles are classified subjectively as to whether they are more observational/applied modeling (light shading) or more theoretical/idealized modeling (dark shading) studies. References were compiled through October 1998. Listings of articles were compiled mainly from literature searches performed by Katherine Day.

numerical-model data and the popularization of CSI diagnostics by forecasters (e.g., Dunn 1988; Lussky 1989; Grumm and Nicosia 1997; Wiesmueller and Zubrick 1998), evaluation of CSI locally at universities, laboratories, and forecast offices is becoming more common. With the relative computational ease of CSI-related parameters and the increasing emphasis on short-term quantitative precipitation forecasting, CSI frequently becomes a default explanation for banded precipitation. 4) Whereas idealized modeling studies of flows possessing CSI have been performed, the applicability of those results to observations may be questionable. Consequently, such theoretical and numerical results often are unappreciated by observational meteorologists. Similarly, observational results usually are not described from a theoretical or numerical-modeling framework. This leads to an ever increasing rift between theory and observations of CSI. Thus, for these four reasons, CSI is commonly observed yet often misinterpreted and misunderstood.

The purpose of this article is twofold: to attempt to limit further misuse of the CSI paradigm by researchers and forecasters alike by highlighting common pitfalls, and to encourage future research explorations that are directed at the deficiencies in our understanding of MSI and slantwise convection. The remainder of this article is as follows. In section 2, we develop parallels between an ingredients-based methodology for forecasting moist gravitational convection (also known as buoyant or upright convection) and slantwise convection. These three ingredients of instability, moisture, and lift are explored further in this article: section 3 reviews the calculation of symmetric instability and section 4 discusses moisture and lift, specifically the relationship between MSI and frontogenesis. In section 5, the implications for the coexistence of instabilities to both moist gravitational and slantwise convections are examined, including a discussion of the structure, evolution, dynamics, and possible electrification of weather systems that might result from such scenarios. Section 6 investigates the nature of cloud and precipitation banding in relation to MSI, and section 7 addresses the diagnosis of slantwise convection using mesoscale numerical-model output. Finally, section 8 consists of a summary of main points, directions for future research, and a concluding discussion.

2. An ingredients-based methodology for slantwise convection

Throughout this article, we wish to differentiate between *free convection* and *forced convection* as motions in the atmosphere that are associated with the presence and absence of instability, respectively (Huschke 1959, 133–134; Emanuel 1980, 192–193). Unless otherwise specified, we use the generic term *convection* to imply *free convection* (gravitational or symmetric).

To clarify some of the confusion surrounding the concepts of CSI and slantwise convection, we find it useful to demonstrate parallels with the more familiar concepts of moist gravitational instability and convection. An exploration of these parallels begins with an ingredients-based methodology for forecasting deep, moist convection (McNulty 1978, p. 664; Doswell 1987, p. 7; Johns and Doswell 1992, 589–590; McNulty 1995, 189–191;

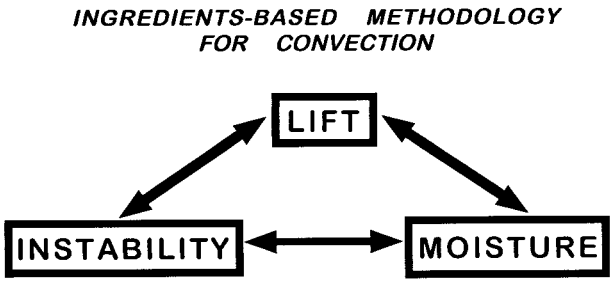

FIG. 2. An ingredients-based methodology for forecasting gravitational or slantwise convection.

Doswell et al. 1996, p. 563). This methodology asserts that three ingredients are required to produce deep, moist convection: instability, moisture, and lift (Fig. 2). As Doswell (1987, p. 7) notes, ''remove any one of these and there well may be some important weather phenomena, but the process is no longer deep, moist convection.''

For the purposes of this article, we adopt the same triad of ingredients from moist gravitational convection (instability, moisture, and lift) for the production of moist slantwise convection, where the requisite instability becomes MSI, rather than moist gravitational instability. Although some previous studies use the ingredients-based methodology implicitly, our interpretation of some of the other previous literature is that CSI is treated sometimes as an instability and sometimes as a forcing mechanism for ascent. An example is illustrated by those who wish to separate the effect of CSI from that due to frontogenesis, when in fact these two processes often cannot be considered independently (see section 4). The ingredients-based methodology firmly labels CSI as the instability, clearly separate from the lifting mechanism.

Applying the ingredients-based methodology to slantwise convection indicates that the existence of CSI alone is not sufficient to initiate slantwise convection. Employing CSI in this manner is tantamount to saying that the occurrence of a severe thunderstorm is due solely to the presence of conditional instability to moist gravitational convection! Since slantwise convection is the process by which the instability is released, it follows that the terms *moist slantwise convection* and *CSI* do not have the same meaning, contrary to their implied equivalence by some authors (e.g., Wolfsberg et al. 1986, p. 1552; Moore and Blakley 1988, p. 2167; Howard and Tollerud 1988, p. 170; Lemaître and Testud 1988, p. 261; Bennetts et al. 1988, p. 368; Emanuel 1990, p. 473; Reuter and Yau 1993, p. 375; Lagouvardos et al. 1993, p. 1293; Grumm and Nicosia 1997, p. 10; Wiesmueller and Zubrick 1998, p. 85; Koch et al. 1998, p. 2040).

In contrast, Thorpe and Rotunno (1989, 1293–1294) have suggested that ''slantwise convection'' is not appropriate terminology to describe the circulations that release CSI. Taking the fluid dynamicists' definition of convection to be a circulation that results in positive heat flux, Thorpe and Rotunno (1989) note that the heat flux with CSI circulations can be negative in certain cases (e.g., Miller 1984), and, hence, these circulations formally should not be considered ''convection.'' These thoughts on terminology, however, are not shared by all in the atmospheric science community. For example, it has been argued that the equations for symmetric instability are isomorphic to both inertial instability and gravitational instability (e.g., Emanuel 1983b, 2016–2017; Xu and Clark 1985; Emanuel 1994, 394–395). Therefore, the release of each instability individually can be considered a form of convection. In agreement with this latter argument, we choose the term slantwise convection to represent the release of MSI.

It should be noted that there are limitations to this analogy between slantwise and gravitational convection. As noted by Emanuel (1990, p. 473), ''the fact that precipitation falls vertically and that turbulence may not be isotropic may serve to make the physics of slantwise convection quite different from that of upright convection, though this has hardly been explored.'' Further discussion of turbulence as it relates to slantwise convection can be found in Emanuel (1994, p. 406).

As is shown throughout this article, the occurrence of slantwise convection depends upon all three ingredients and all must be present in order to justify any claims of slantwise convection. Next, in section 3 we examine how symmetric instability is evaluated. Moisture and lift are discussed in section 4.

3. Assessing symmetric instability

The derivation of dry and moist symmetric instability is not presented here. Interested readers are referred to the following sources for further information. Early work on symmetric instability by Helmholtz, Rayleigh, Solberg, Bjerknes and Godske, Kleinschmidt, Fjørtoft, Sawyer, Eliassen, Kuo, Ooyama, Stone, McIntyre, and others is reviewed by van Mieghem (1951), Emanuel (1979), Xu (1986b), and Shutts (1990). The basics of dry symmetric instability are presented in Lilly (1986), Holton (1992, section 9.3), and Bluestein (1993, 339–350). Derivations of MSI can be found in the pioneering works of Bennetts and Hoskins (1979) and Emanuel (1983a,b), or the excellent textbook presentations of Bluestein (1993, section 3.5.2), Houze (1993, section 2.9.1), and Emanuel (1994, chap. 12).

a. Dry symmetric instability

Dry symmetric instability is a generalization of both inertial instability and dry gravitational instability. The term *symmetric* refers to a basic state and perturbations that are independent of a horizontal direction, here assumed to be parallel to the *y* axis. Table 1 compares gravitational, symmetric, and inertial instabilities, illustrating the parallelism in their definitions and measures.

TABLE 1. Definitions of different types of stabilities (Northern Hemisphere): † = at saturation, $\overline{\theta}_e = \overline{\theta}_e^*$; ‡ = $\overline{\theta}_w$ can be used equivalently for $\overline{\theta}_e$.

	Gravitational	Symmetric	Inertial
Dry	Absolute instability	Symmetric instability	Inertial instability
	$\dfrac{d\overline{\theta}}{dz} < 0$	$\left.\dfrac{d\overline{\theta}}{dz}\right\|_{M_g} < 0; \quad \left.\dfrac{dM_g}{dx}\right\|_{\overline{\theta}} < 0$	$\dfrac{dM_g}{dx} < 0$
	$-\dfrac{dT}{dz} > \Gamma_d$	$-\left.\dfrac{dT}{dz}\right\|_{M_g} > \Gamma_d\|_{M_g}$	$\zeta_g + f < 0$
		M_g–$\overline{\theta}$ relationship	
		$\mathrm{PV}_g < 0$	
Conditional†	Conditional instability (CI)	Conditional symmetric instability (CSI)	N/A
	$\dfrac{d\overline{\theta}_e^*}{dz} < 0$	$\left.\dfrac{d\overline{\theta}_e^*}{dz}\right\|_{M_g} < 0; \quad \left.\dfrac{dM_g}{dx}\right\|_{\overline{\theta}_e^*} < 0$	
	$\Gamma_m < -\dfrac{dT}{dz} < \Gamma_d$	$\Gamma_m\|_{M_g} < -\left.\dfrac{dT}{dz}\right\|_{M_g} < \Gamma_d\|_{M_g}$	
		M_g–$\overline{\theta}_e^*$ relationship	
		$\mathrm{MPV}_g^* < 0$	
Potential‡	Potential instability (PI)	Potential symmetric instability (PSI)	N/A
	$\dfrac{d\overline{\theta}_e}{dz} < 0$	$\left.\dfrac{d\overline{\theta}_e}{dz}\right\|_{M_g} < 0; \quad \left.\dfrac{dM_g}{dx}\right\|_{\overline{\theta}_e} < 0$	
		M_g–$\overline{\theta}_e$ relationship	
		$\mathrm{MPV}_g < 0$	

As noted by Jones and Thorpe (1992, p. 231), ''at the present time, symmetric instability theory is applicable only to two-dimensional flow.'' Therefore, when applying this theory to observational data, it must be remembered that a three-dimensional perturbation on such a flow may not necessarily release the instability, an issue dealt with in more detail by Jones and Thorpe (1992) and Gu et al. (1998).

In the Northern Hemisphere (assumed throughout this article), the condition for inviscid, inertial instability is $\partial M_g/\partial x < 0$, where $M_g = v_g + fx$ is the *geostrophic absolute momentum* (also known as *geostrophic pseudoangular momentum*) of a geostrophically balanced mean state, v_g is the geostrophic wind in the direction perpendicular to the temperature gradient (hereafter, the alongfront direction, although strictly we are considering a baroclinic zone, not necessarily a front), f is the Coriolis parameter, and x is the cross-front distance, increasing toward warmer air. This condition is equivalent to the geostrophic absolute vorticity being negative. Similarly, the condition for inviscid, dry gravitational instability (what is typically referred to as *dry absolute instability* by meteorologists) is that the hydrostatically balanced mean-state potential temperature $\overline{\theta}$ decreases with height z (i.e., $\partial\overline{\theta}/\partial z < 0$).

Whereas a parcel may be inertially stable to horizontal (constant z) displacements ($\partial M_g/\partial x > 0$) and gravitationally stable to vertical displacements ($\partial\overline{\theta}/\partial z > 0$) separately, it may be unstable with respect to *slantwise* displacements by dry symmetric instability. The condition for dry symmetric instability is that M_g surfaces slope less steeply than $\overline{\theta}$ surfaces (hereafter called *the M_g–$\overline{\theta}$ relationship*). Dry symmetric instability can be viewed as either dry gravitational instability on a M_g surface (i.e., $\partial\overline{\theta}/\partial z|_{M_g} < 0$) or inertial instability on an isentropic surface (i.e., $\partial M_g/\partial x|_{\overline{\theta}} < 0$). Therefore, any slantwise displacement that occurs at an angle between the slopes of the M_g and $\overline{\theta}$ surfaces will release the symmetric instability.

In the strictest sense, symmetric instability should be determined relative to these hydrostatically and dynamically (in this case, geostrophically) balanced mean states. [See Persson and Warner (1995, 3457–3458) and Xu (1992, p. 632) for further discussion of this point.] Since the atmosphere is hydrostatic to a very good approximation, using the environmental potential temperature θ instead of $\overline{\theta}$ probably introduces minimal error. In general, though, the atmosphere is not geostrophic and may, in fact, exhibit large departures from geostrophy in regions susceptible to symmetric instability (e.g., Seltzer et al. 1985, section 3c; Wolfsberg et al. 1986, p. 1553; Knight and Hobbs 1988, p. 926; Byrd 1989, 1128–1129). In observational studies that assess symmetric instability from limited observations such as single soundings, the geostrophic wind is often approximated by the total wind and stated explicitly as such (e.g, Emanuel 1983b, 1988; Byrd 1989; Reuter and Aktary 1995). An additional complication occurs with mesoscale-model data in which the geostrophic wind (derived from the geopotential height) is often much noisier

than the total wind (Shutts 1990, p. 2747), although methods have been developed to construct well-behaved fields from numerical-model data (e.g., Barnes et al. 1996). In time, more researchers and forecasters are approximating M_g by M (i.e., $M = v + fx$, where M is the absolute momentum calculated from the total along-front wind v), interchanging the total wind v for the geostrophic wind v_g, even when the geostrophic wind is readily available (e.g., Martin et al. 1992; Leach and Kong 1998; Chen et al. 1998).

The use of M instead of M_g is inconsistent with the theory for symmetric instability discussed above. If significant flow curvature is present (especially changes in curvature in the vertical), the observed alongfront wind v is better approximated by the alongfront gradient wind v_{gr} rather than the alongfront geostrophic wind v_g. Sanders (1986, section 4b) derives the condition for symmetric instability relative to a basic state in gradient-wind balance and presents nomograms for its use. That condition is $-3\overline{v}_{gr}(1 + \overline{v}_{gr}/fr)/r < 0$, where $\overline{v}_{gr}$ is the basic-state alongfront gradient-wind speed and r is the distance along the radius of curvature.

By using the observed wind to compute M, rather than the geostrophic wind, situations with strong cyclonic shear (near-horizontal M surfaces) may be assessed to be more ''inertially'' stable to ascent along a $\overline{\theta}$ surface than they really are, since the computed M surface includes the additional balance provided by the centrifugal force. In addition, in areas with orography, large pressure changes, or intense frontogenesis, significant ageostrophy in the observed lower-tropospheric wind can occur. In those cases, the geostrophic wind may be unidirectional but the observed wind may have significant curvature (and not be nearly two-dimensional). Extensions of this theory to these situations of questionable two-dimensionality are considered in section 3c.

Therefore, to assess the condition for dry symmetric instability, replacing the hydrostatically balanced basic state $\overline{\theta}$ by θ is generally a valid approximation. Hereafter, throughout this article, we approximate $\overline{\theta}$ by θ. In contrast, replacing the geostrophically balanced basic state M_g by M may be a poor approximation, but this subject has not been addressed extensively in the literature. For example, in some situations, while the observed wind may not be similar to the geostrophic wind, their vertical gradients, the factor important in calculating M/M_g, may be more similar. Until further investigation is performed to evaluate the importance of this assumption, we recommend use of the geostrophic wind.

A final point is that separating the data (observations or model-derived) into basic state and perturbation is a complicated issue in its own right (i.e., the so-called partitioning problem). In practice, the geostrophic wind is usually computed directly from the total pressure or height field. This implicitly assumes that the perturbation pressure caused by the unbalanced part of the flow (such as gravitational convection, MSI circulations, and gravity waves) is negligible, an assumption that may not be valid after these perturbations are already present. In this case, how to partition the total flow is not a trivial matter, especially when CSI is evaluated in three-dimensional space with an extended criterion applied to geostrophic flow (e.g., Shutts and Cullen 1987) or other nonlinearly balanced flow (e.g., Xu 1994, appendix C). How, and even whether, to perform the partition and what balanced system to use (e.g., geostrophy, gradient-wind balance, semigeostrophy, or higher-accuracy dynamical system) remain difficult questions. Even if complete data are available for performing a partition in space and time, the partition may not be precisely or uniquely determined. Unfortunately, our understanding of these issues is still very limited and may profoundly affect our assessment of symmetric stability from atmospheric observations. If, however, such complicated partitions are deemed necessary in order to assess MSI rigorously, they are unlikely to become operationally feasible.

b. Moist symmetric instability: Conditional symmetric instability versus potential symmetric instability

The addition of moisture complicates the theory of symmetric instability considerably. For moist gravitational convection, conditional instability (CI) occurs locally at each height along a vertical sounding where the environmental lapse rate lies between the moist- and dry-adiabatic lapse rates, or, equivalently, θ_e^*, the *saturation equivalent potential temperature*,[1] decreases with height (i.e., $\partial\theta_e^*/\partial z < 0$). Similarly, for slantwise convection, CSI occurs locally at each height where the environmental lapse rate along a M_g surface lies between the moist- and dry-adiabatic lapse rates (i.e., is conditionally unstable along a M_g surface), or $\partial\theta_e^*/\partial z|_{M_g} < 0$. The instability is said to be *conditional* because saturation must be present locally in order for air parcels to be unstable (i.e., possess parcel buoyancy).[2]

Contrast these definitions for conditional instabilities

[1] Also expressed as θ_{es} in some literature, $\theta_e^* = \theta \exp(Lq_{vs}/c_pT)$, where L is the latent heat of vaporization, q_{vs} is the saturation mixing ratio, c_p is the specific heat of dry air at constant pressure, and T is the air temperature (e.g., Houze 1993, p. 54). The saturation equivalent potential temperature is the equivalent potential temperature the air would have if it were saturated with water at the same pressure and temperature. When the air is not saturated, θ_e^* is not conserved, but when the air is saturated, $\theta_e = \theta_e^*$ and, hence, both are conserved.

[2] It was noted during review of this article that the revised version of the *Glossary of Meteorology* will include two definitions for *conditional instability* (K. Emanuel 1998, personal communication). The first definition is the standard one described above [i.e., the environmental lapse rate lies between the moist and dry adiabatic lapse rates (Huschke 1959, p. 125)]. The second definition is a state of positive convective available potential energy (CAPE). The revision was deemed necessary because (a) the standard definition does not necessarily imply a reservoir of potential energy for convection, and (b) operational usage of the term conditional instability relies more on measures of parcel buoyancy like CAPE or the lifted index.

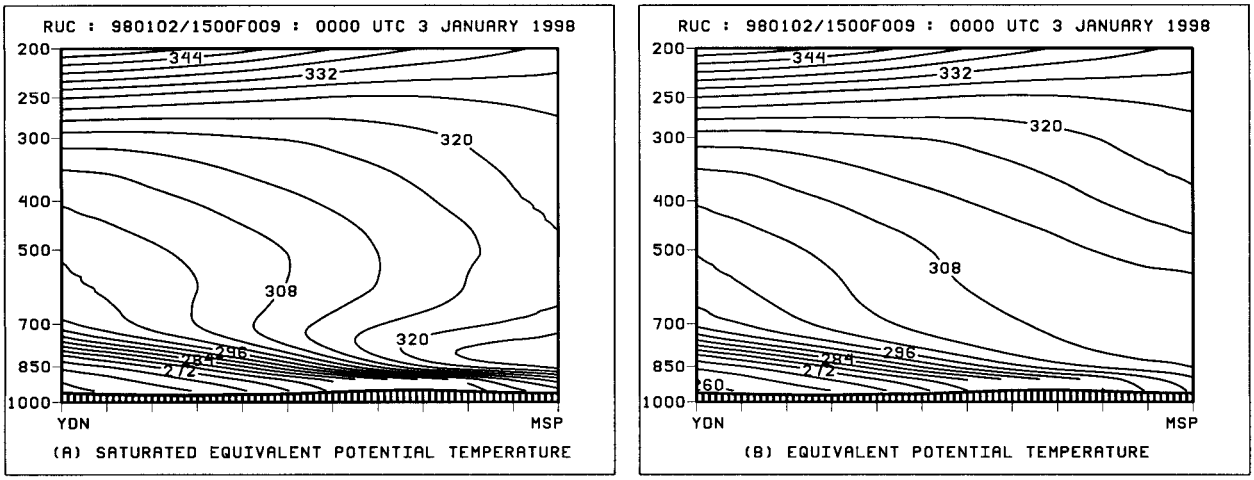

FIG. 3. Rapid Update Cycle (RUC) 9-h forecast verifying 0000 UTC 3 Jan 1998. Cross section from Dauphin, Manitoba (YDN), to Minneapolis–St. Paul, Minnesota (MSP): (a) saturated equivalent potential temperature θ_e^* (solid, every 4 K); (b) equivalent potential temperature θ_e (solid, every 4 K).

to those for potential instabilities. The difference between CI and PI has been discussed by, for example, Wallace and Hobbs (1977, section 2.7.3), Rogers and Yau (1989, p. 35), and Emanuel (1994, p. 185). As in moist gravitational convection where the potential instability (PI; also known as convective instability) of a layer along a vertical sounding can be defined ($\partial\theta_e/\partial z < 0$), it is possible to assess layer potential symmetric instability (PSI) along a M_g surface: $\partial\theta_e/\partial z|_{M_g} < 0$. The instability is said to be *potential* because the potentially unstable layer first must undergo a finite vertical displacement to reach saturation and *create* the instability; release of the instability may then result, given sufficient forcing for ascent. It can be shown that the criterion for PSI is equivalent to the M_g–θ_e relationship. Therefore, *the commonly employed method of assessment for CSI in the literature, the M_g–θ_e relationship, is really a measure of PSI, not CSI, if we follow the definitions from moist gravitational convection.*

Strictly, the saturation equivalent potential temperature θ_e^* should be used to assess CSI, as noted by several authors (Emanuel 1988; Reuter and Yau 1990, p. 449; Thorpe and Clough 1991; Houze 1993). There can be a substantial difference between θ_e^* and θ_e, as illustrated by Fig. 3, a cross section across an equatorward-moving lower-tropospheric cold front over the northern United States. Although the air above the frontal surface is conditionally unstable since θ_e^* decreases with height (Fig. 3a), it is potentially stable since θ_e increases with height (Fig. 3b). This case illustrates the importance of recognizing possible differences between θ_e^* and θ_e and its relationship to assessing MSI.

The wet-bulb potential temperature θ_w is also a conserved variable under dry- and pseudoadiabatic processes and may be equivalently employed for θ_e in diagnosing PSI. At saturation, the vertical gradients of θ_e, θ_e^*, and θ_w are equivalent, therefore, CI and PI, as well as CSI and PSI, are equivalent. More will be said about determining saturation using observational data and mesoscale models in sections 4 and 7.

It is surprising to note that this misnomer of CSI has deep roots and likely arises from later authors' misinterpretation of the original work. Bennetts and Hoskins (1979, 949–951) define CSI for a ''two-dimensional flow in an atmosphere which is assumed to be saturated everywhere'' as a natural extension of CI, which they define as the wet-bulb potential temperature decreasing with height. As mentioned previously, CI and PI are equivalent concepts only when the atmosphere is saturated. Thus, many later researchers and forecasters continue to use θ_e/θ_w and the term CSI, but may not realize the assumption of saturation, explicitly stated by Bennetts and Hoskins (1979). Also, meteorologists' familiarity with θ_e as a tracer of dry and irreversible moist processes and the ability to compute θ_e readily in meteorological analysis packages probably facilitate the use of θ_e over θ_e^* in assessing MSI.

Despite the fact that several authors define and use CSI correctly in their own work (e.g., Reuter and Yau 1990, p. 449; Houze 1993, 54–56; Emanuel 1994, p. 410), this misuse of the term CSI continues and now pervades the literature. We would like to suggest that, in the future, we, as a meteorological community, use the term CSI only when employing θ_e^* and use the term PSI only when employing θ_e. We adopt this terminology throughout the rest of the article. In addition, we use the term MSI when the method of assessment is unimportant or is not specified.

The question naturally arises as to whether it is more appropriate to calculate CSI or PSI for assessing the possibility of moist slantwise convection in the atmosphere. Drawing an analogy to moist gravitational convection may help provide some insight. The necessary condition for moist gravitational convection is that a

rising air parcel be saturated and the lapse rate be greater than the moist adiabatic lapse rate (CI), so that positive buoyancy exists. Meeting the lapse-rate requirement for PI or PSI is only a necessary condition for release of the instability; saturation must also occur. Consequently, the presence of PI is not necessary for moist gravitational convection to occur in the atmosphere (e.g., Emanuel 1994, p. 185). Therefore, throughout the rest of this article, we use the term CSI, computed with the proper thermodynamic variable θ_e^*, as the appropriate measure of the susceptibility of the atmosphere to slantwise convection. Thus, many previous studies may not determine the true potential for slantwise convection because of their use of θ_e and PSI, rather than θ_e^* and CSI.

c. The validity of the M_g–θ_e relationship and moist geostrophic potential vorticity

Certain assumptions are necessary in order to develop the M_g–θ_e^* relationship for the identification of CSI: 1) the geostrophic wind is constant in the alongfront direction, 2) the cross section for evaluating the M_g–θ_e^* relationship is perpendicular to the vertical shear of the geostrophic wind (or, equivalently, the thermal wind or isotherms), and 3) the ageostrophic wind (e.g., due to flow curvature) is small so that the geostrophic wind is a reasonable approximation to a basic state. Discrepancies in interpreting the existence of CSI in cross sections can result, therefore, because one or more of the above criteria is not strictly met. Further discussion of this point, and the extension to three dimensions of the M_g–θ_e relationship for assessing PSI, is found in Shutts and Cullen (1987) and Shutts (1990).

It can be shown that extending the M_g–θ relationship for dry symmetric instability to three dimensions is equivalent to computing geostrophic potential vorticity PV_g (e.g., Hoskins 1974), where $\mathrm{PV}_g = g\boldsymbol{\eta}_g \cdot \nabla\theta$, g is gravity, $\boldsymbol{\eta}_g$ is the three-dimensional geostrophic absolute vorticity vector, and ∇ is the gradient operator in x, y, and z coordinates. When PV_g is negative (and inertial and dry gravitational instabilities are absent), dry symmetric instability is present. Likewise, the three-dimensional form of the M_g–θ_e^* relationship for CSI is equivalent to negative saturated geostrophic potential vorticity MPV_g^* (also known as the saturated equivalent geostrophic potential vorticity, $\mathrm{MPV}_g^* = g\boldsymbol{\eta}_g \cdot \nabla\theta_e^*$), when inertial and conditional instabilities are absent. Also, the three-dimensional form of the M_g–θ_e relationship for PSI is equivalent to negative moist geostrophic potential vorticity $\mathrm{MPV}_g = g\boldsymbol{\eta}_g \cdot \nabla\theta_e$, when inertial and potential instabilities are absent. Therefore, assessing CSI using the three-dimensional form of MPV_g^* does not require strict adherence to the same assumptions as using the M_g–θ_e^* relationship in cross-section form. Owing to the potential confounds with assessing M_g–θ_e^* relationships in cross sections, a more reliable assessment of CSI is obtained by employing MPV_g^* or another equivalent three-dimensional parameter. On the other hand, use of $\mathrm{MPV}_g/\mathrm{MPV}_g^*$ as a diagnostic tool does not differentiate between regions of PI/CI and PSI/CSI (e.g., McCann 1995; Wiesmueller and Zubrick 1998, 94–95). Likewise, regions of inertial instability and convective stability may also indicate negative $\mathrm{MPV}_g/\mathrm{MPV}_g^*$. Therefore, MSI diagnostics always should be employed in conjunction with tests for moist gravitational and inertial instabilities. Further discussion of this point is found in section 5. Other three-dimensional parameters that are used to assess MSI include a growth-rate parameter (e.g., Bennetts and Hoskins 1979, p. 952; Bennetts and Sharp 1982, p. 596), a moist Richardson number [e.g., Sanders and Bosart 1985, Eq. (4); Seltzer et al. 1985], and a moist symmetric-stability parameter (e.g., Jascourt et al. 1988, p. 181).

From the three-dimensional form of MPV_g, Moore and Lambert (1993) derive a two-dimensional form of MPV_g [their Eq. (2)] and use it to assess PSI in their cross sections. Consequently, their results depend upon the orientation of the cross section as in the M_g–θ_e relationship (i.e., the full potential of MPV_g as a three-dimensional parameter for diagnosis is not being utilized). Thus, even in cross sections, application of the full three-dimensional form of MPV_g is essential for an accurate assessment of PSI. Unfortunately, employing the two-dimensional form of MPV_g has been increasing in popularity (e.g., Weisman 1996; Wiesmueller and Zubrick 1998).

d. Slantwise convective available potential energy

Analogous to convective available potential energy (CAPE) for gravitational convection (e.g., Emanuel 1994, 169–172), slantwise convective available potential energy (SCAPE) can be defined (e.g., Emanuel 1983b, sections 2 and 3; Shutts 1990; Emanuel 1994, 407–409). These parameters measure the amount of positive area on a thermodynamic diagram and represent the maximum kinetic energy possible from adiabatic, inviscid parcel theory. In the case of CAPE, it is the maximum kinetic energy of a vertical updraft; in the case of SCAPE, it is the maximum kinetic energy of an updraft along a M_g surface,[3] consisting of *both* horizontal and vertical motions, contrary to Black et al. [1994, their Eq. (11); although their later assumption that $\partial\theta_e/\partial z = 0$ mitigates this discrepancy] and McCann (1996, p. 122), who use SCAPE as a measure of vertical motion only.

The use of SCAPE as a measure of the potential for slantwise convection has not been particularly common in the literature, despite the similarity to its more popular relative CAPE. Byrd (1989) finds that values of SCAPE

[3] When the air motion is not along the M_g surface, the upper bound of available energy can be estimated by the generalized energetics of Xu (1986b).

were of limited value in determining the degree of banding within precipitating regions over the southern Plains, whereas Shutts (1990) shows that values of SCAPE derived from mesoscale numerical-model output are somewhat related to explosive cyclogenesis over the North Atlantic Ocean. Most other examples in the literature involve the computation of SCAPE for individual cases and therefore cannot be placed within a broader context relative to other events. The lack of studies on SCAPE makes its interpretation as a diagnostic tool uncertain, but can also be viewed as SCAPE not being a particularly useful parameter. These issues are compounded by 1) the difficulty in computing SCAPE from upper-air observations, 2) the relatively small values of SCAPE typically observed in regions of active slantwise convection (see section 4), and 3) the small values of SCAPE in comparison to CAPE, when CAPE is zero or small. These difficulties make further investigation of the utility of SCAPE difficult (McCarthy 1996), probably limiting more widespread usage.

e. Neglected effects

It is important to note that the concept of MSI, like gravitational instability, is based upon parcel theory. Therefore, the caveats and limitations with using parcel theory for gravitational convection also apply to using parcel theory for slantwise convection. [For further discussion on parcel theory as applied to symmetric instability, see Thorpe et al. (1989).] In particular, assumptions about mixing and microphysical processes strongly affect computations of parcel buoyancy.

One example is the weight of condensed water on buoyancy (also known as water loading). Reuter and Yau (1993), following the methodology of Xu and Emanuel (1989), find that soundings exhibiting MSI are actually neutral or stable to moist slantwise ascent when the effects of water loading on the virtual temperature are included. To include the effects of water loading, however, the assumption must be made that all condensed water remains with the parcel, an assumption that obviously fails in precipitating clouds and may fail in other situations as well (Xu and Emanuel 1989, section 5). Williams and Renno (1993) find that, if water loading is included, then logically this water must be frozen, if it reaches sufficient height. They find that the additional positive buoyancy due to release of this latent heat of fusion more than offsets the negative buoyancy due to water loading. Therefore, both contributions, or neither contribution, should be considered when assessing parcel buoyancy.

Correction factors for ice-phase transitions (e.g., Reuter and Beaubien 1996; Rivas Soriano and García Díez 1997) and sphericity terms (Shutts 1990, p. 2747) also may be included to assess MSI, but these generally are not performed. Doswell and Rasmussen (1994), in an approach distinct from Xu and Emanuel (1989), present arguments for neglecting some of these effects in the calculation of CAPE from observations, while retaining the correction for virtual temperature. Since the use of CAPE/SCAPE from a forecasting perspective does not require numerical precision, these additional corrections are probably not necessary. If numerical precision is required, however, all effects should be accounted for. In this article, we have not included explicitly the virtual-temperature correction for simplicity, but we recognize that, for certain applications (e.g., warm-season events, deep tropospheric circulations), it should be incorporated.

f. The absence of instability

Finally, if both adequate moisture and lift are present in the absence of MSI, such that ascending air is forced to its condensation level and beyond (forced convection), banded clouds may still form, with heavy precipitation being the result [e.g., the case presented in Doswell et al. (1998, section 3c)]. Forced slantwise ascent leading to a single cloud/precipitation band can occur in the absence of MSI over a mountain due to orographic lift or over a frontal zone due to secondary circulations associated with frontogenesis, but this is not free convection. When MPV_g is positive, multiple bands can be generated externally only by preexisting PV_g or MPV_g anomalies (e.g., Chan and Cho 1989; Cho and Chan 1991; Xu 1992). Observational documentation of these features, however, has not occurred. Therefore, the absence of MSI does not preclude the formation of single- or multiple-banded clouds and precipitation, much as the absence of potential or conditional instability to moist gravitational convection does not preclude the same.

g. Assessing MSI from observations

Although numerous studies have used observations to assess MSI, difficulties arise in doing so [see, e.g., Persson (1995, section 2)]. For instance, the assessment of MSI is sensitive to moisture, a variable with strong spatial gradients and not measured with the same resolution or accuracy as pressure, temperature, and wind. Another difficulty is that the typical spacing of M_g surfaces is less than the spacing between upper-air stations, such that the horizontal variations in thermodynamic variables along M_g surfaces are poorly resolved. To deal with these limitations, previous researchers have resorted to using a single observational sounding and assuming geostrophy (e.g., Emanuel 1983b; Byrd 1989), estimating the vorticity with height (e.g., Seltzer et al. 1985; Reuter and Aktary 1993), or taking direct observations along M surfaces using aircraft (Emanuel 1988).

Also, like gravitational instability, the rapid timescale of adjustment to slantwise neutrality is believed to occur very quickly ($\sim$3 h or less), meaning that standard atmospheric observations will not capture the thermodynamic structure of the adjustment. Therefore,

conclusions about many of the details involved in slantwise convection necessarily must be inferred. Using gridded numerical datasets from objective analysis or mesoscale models may appear to sidestep these issues, but the use of these datasets presents its own problems (see section 7). The analyst must be able to recognize the limitations of the particular dataset chosen and act accordingly.

4. Frontogenesis and MSI

The eventual release of MSI is predicated upon slantwise parcel lifting beyond the lifting condensation level to the level of free slantwise convection (LFSC). Therefore, saturation must be present in the region of slantwise ascent in order for the instability to be released. Typically, previous authors examine the relative humidity and if it is greater than some threshold (say, 80%), then saturation is considered to have occurred or is imminent. This value is smaller than 100% to account for data errors, inadequacies in the model (see section 7), and/or saturation with respect to ice.

The ascent required to lift a parcel forcibly to its LFSC can arise from frontogenetical circulations, traveling meso- or synoptic-scale systems, orography, or any other mechanism of sufficient magnitude. Doswell (1987, p. 7) has argued that synoptic-scale ascent probably is not responsible for initiation of deep, moist gravitational convection. On the other hand, slantwise convection occurs on slightly larger scales than gravitational convection. Therefore, resolving the processes responsible for lift on the meso-α and synoptic scales (greater than 200 km) is likely in most cases of suspected MSI. The relative roles of synoptic and mesoscale processes in the initiation of gravitational and slantwise convection are poorly known, compounding the difficulty in understanding convective initiation (Ziegler and Rasmussen 1998). The details of convective initiation, however, are beyond the scope of this review.

In comparing observations to idealized models, it is useful to draw the distinction between the release of MSI occurring due to the growth of infinitesimal perturbations (i.e., normal-mode theory) and the release of MSI occurring in the presence of some larger-scale forcing (i.e., frontogenesis, orographical circulations, etc.). Fischer and Lalaurette (1995a,b) compare these scenarios, finding that idealized normal-mode simulations produce growth rates that are too slow [$\sim(11\ \text{h})^{-1}$] to account for observed features. Also, weaker vertical velocities develop in the normal-mode simulations compared to simulations of MSI with frontogenesis. Strong forcing (say, in the form of frontogenesis) is required to overcome two factors that inhibit the release of MSI: turbulent diffusion in the narrow, moist ascent and the resistance of the positive buoyancy in the broader, dry, compensating subsidence. Therefore, finite-amplitude forcing is usually considered to be present for the release of MSI in the real atmosphere (see also Innocentini and dos Santos Caetano Neto 1992). These studies support the observation that few examples of MSI in the absence of frontogenesis exist [a possible exception is Wood and Nielsen-Gammon (1994)].

Because both frontogenesis and slantwise convection due to the release of MSI produce banded precipitation, some authors try to distinguish between banded precipitation purely due to frontogenetical forcing from those purely due to the release of MSI (e.g., Seltzer et al. 1985; Snook 1992; Rauber et al. 1994). We argue in this section that the atmospheric response in an environment characterized by MSI is typically closely related to the frontogenetic forcing, making this separation intractable (Thorpe and Emanuel 1985, 1821–1822; Emanuel 1994, p. 412).

First, numerous published observational examples demonstrate the simultaneous presence of weak symmetric stability and frontogenesis, suggesting that slantwise neutrality has been reached. The most convincing of these studies include Emanuel (1983b, 1988), Sanders and Bosart (1985), Sanders (1986), Colman (1990a,b), Reuter and Yau (1990), Thorpe and Clough (1991), Locatelli et al. (1994), Kristjánsson and Thorsteinsson (1995), Huo et al. (1995), and Loughe et al. (1995). The idealized-modeling studies of Emanuel (1985), Thorpe and Emanuel (1985), and Xu (1989b) clarify the relationship between symmetric instability and frontogenesis, implicit in the Sawyer–Eliassen equation for secondary frontal circulations. [Reviews of the Sawyer–Eliassen equation can be found in Bluestein (1986), Eliassen (1990), and Keyser (1999).] In the Sawyer–Eliassen equation, the symmetric stability (through PV_g) modulates the atmospheric response to the forcing (i.e., the same forcing produces narrower, stronger ascent in an environment of weaker symmetric stability than in an environment of stronger symmetric stability). As such, separating the contributions to ascent from the release of MSI versus frontogenesis is not possible within the framework of the Sawyer–Eliassen equation.

Second, as discussed in Emanuel (1994, sections 11.2 and 12.3) and Mapes (1997), it is useful to consider two types of (gravitational or slantwise) convection: activated (or triggered) and statistical-equilibrium. Activated convection requires a buildup of available potential energy before the convection is ''triggered'' by some lifting mechanism, thereby releasing the instability. Statistical-equilibrium convection, on the other hand, is a process by which the consumption of available potential energy due to convection occurs as physical processes, such as differential horizontal thermal advection in the vertical, tend to destabilize the atmosphere. Thus, statistical-equilibrium convection occurs in an environment in which CAPE/SCAPE is relatively constant in time.

Whereas activated moist gravitational convection is

commonly observed in the atmosphere, clear observational signatures of activated slantwise convection are not as readily identifiable. In activated moist gravitational convection, the buildup of large CAPE is often aided by the presence of a low-level capping inversion, which is eventually penetrated by surface-based ascent leading to the release of the instability. Therefore, by analogy, activated moist slantwise convection would be indicated by a region of SCAPE prior to the onset of slantwise convection. Few studies, however, thoroughly document the conditions before slantwise-convective initiation.

In contrast, statistical-equilibrium slantwise convection appears to be more commonly observed than activated slantwise convection (Emanuel 1994, 410–412), particularly along frontal zones, where increases in SCAPE are nearly offset by the consumption of SCAPE by ascent along the frontal zone. A notable example is Wolfsberg et al. (1986), in which geostrophic differential lapse-rate advection maintains the MSI over 12–24 h, even in the presence of continued slantwise ascent. In fact, slantwise convection may appear to persist for many hours after moist symmetric neutrality is reached, suggesting that frontogenesis may continue to force ascent (e.g., Sanders and Bosart 1985; Saitoh and Tanaka 1987; Lemaître and Testud 1988).[4] Many cases of near-slantwise neutrality appear to support the existence of presumed slantwise convection in the presence of frontogenesis (previously listed); large negative values of MPV_g are not observed and the M_g and θ_e surfaces are nearly parallel, suggesting that equilibration is likely to be rather efficient. Indeed, Reuter and Yau (1990) claim that the observed adjustment time is 3 h or less, consistent with the rapid equilibration time (f^{-1}) from scaling arguments (Emanuel 1983b, p. 2032). It should be reiterated that statistical-equilibrium slantwise convection does not need to imply that SCAPE is zero necessarily, only that it is relatively constant. Consequently, measures of PSI may be more appropriate than measures of CSI in these situations.

Finally, for moist gravitational convection, the nature of the large-scale forcing and the response (resulting circulation), and the timescales over which they operate, are so different (hours vs minutes, respectively) that it is relatively easy to separate forcing from response. In contrast, for slantwise convection, timescales for frontogenesis and the release of MSI are more similar (hours), making this scale separation more difficult.

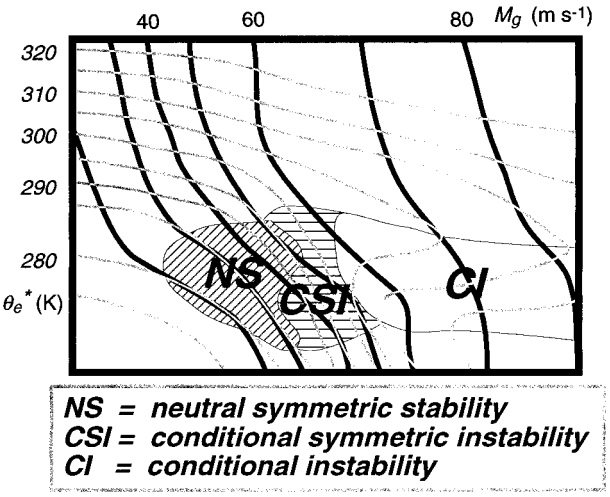

FIG. 4. Stability regimes often observed near frontal zones. Contours represent typical values often present: M_g (thick black lines) and θ_e^* (thin gray lines). Based on a figure originally constructed by James Moore and Sean Nolan.

5. The coexistence of moist gravitational and moist symmetric instabilities

It is often observed in the atmosphere that regions of moist gravitational instability (CI or PI) may be in the same vicinity as regions of MSI (CSI or PSI) (e.g., Emanuel 1983b, Fig. 6; Bennetts and Ryder 1984, Fig. 8; Donaldson and Stewart 1989, Figs. 8 and 13; Thorpe and Clough 1991, Fig. 2; Lemaître and Scialom 1992, Fig. 12; Martin et al. 1992, Fig. 10; Snook 1992, Fig. 10; Reuter and Yau 1993, Figs. 6, 9, 11, and 13; Lagouvardos et al. 1993, Figs. 7–8; Martin 1998, Figs. 8a, 11a, and 12a). For example, a typical stability profile across a frontal environment is illustrated schematically in Fig. 4, based on an unpublished design by J. Moore and S. Nolan. In the warm sector, CI may exist, whereas closer to the front, CSI, symmetric neutrality, and weak symmetric stability may be present (Fig. 4).

As discussed in section 3b, CI is a special case of CSI in which θ_e^* surfaces not only tilt more steeply than M_g surfaces, but are overturned, such that $\partial\theta_e^*/\partial z < 0$. Likewise, PI is a special case of PSI in which θ_e surfaces not only tilt more steeply than M_g surfaces, but are overturned, such that $\partial\theta_e/\partial z < 0$. As such, blindly employing the tests for CSI ($\mathrm{MPV}_g^* < 0$ and the M_g–θ_e^* relationship) will identify regions of CI and blindly applying the tests for PSI ($\mathrm{MPV}_g < 0$ and the M_g–θ_e relationship) will identify regions of PI. Whereas there have been some attempts to discriminate between situations characterized by CI/PI from those characterized by CSI/PSI (Bennetts and Sharp 1982, 598–599; Moore and Lambert 1993; Wiesmueller and Zubrick 1998, p. 86), this distinction is not always made (e.g., Gyakum 1987, p. 2339; Lemaître and Scialom 1992, Fig. 12; Lagouvardos and Kotroni 1995, Fig. 10; Chen et al. 1998, Fig. 21) or is made, but not applied properly (e.g.,

[4] It may be that if MSI is small and negative, then the circulation may approach that of the linear MSI modes, whereas if the statistical-equilibrium slantwise convection manifests highly nonlinear motions, the circulations may be strongly affected or maintained by other processes such as frontogenesis (Q. Xu 1998, personal communication).

Moore and Blakley 1988, p. 2170, Fig. 19; Wang et al. 1990, Figs. 1 and 8; Shields et al. 1991, 956–959; Davidson et al. 1998, p. 1623).[5]

That MPV_g can be used to identify PI and PSI led McCann (1995, p. 801) to refer to MPV_g as an ''all-purpose convection diagnostic tool'' to locate regions where the atmosphere is susceptible to moist gravitational or symmetric instability, seemingly without regard to the nature of any resulting convection. Not considering the distinction between CI/PI, CSI/PSI, and inertial instability leads to nonsensical statements such as, ''the conditions for CSI are satisfied . . . via inertial and conditional *instability*, rather than through inertial and conditional *stability*. . . .'' (Davidson et al. 1998, p. 1623; italics are present in the original citation). Furthermore, McCann's (1995, p. 801) statement that ''the effects of equal CAPE and SCAPE are probably about the same, since parcel accelerations are equal'' implies that vertical and horizontal accelerations of similar magnitudes produce similar dynamics in the atmosphere, a misinterpretation of the differing dynamics of moist gravitational and symmetric instabilities (see section 3d). To be precise, we strongly recommend assessing CI/PI and inertial instability prior to assessing CSI/PSI, in any given case.

a. Convective–symmetric instability

Ultimately, a deeper understanding of how convection (gravitational, slantwise, or both) organizes in the presence of both CI/PI and CSI/PSI is sought. We should note that Xu and Clark (1985) argue for a continuum between gravitational and slantwise convection, so, in a sense, the distinction that is drawn between gravitational and slantwise convection can be considered arbitrary. As further noted by Jones and Thorpe (1992, p. 242), ''the strong distinction which is often made between flows with positive and negative potential vorticity is an artefact [sic] of the use of balanced equations, rather than a physical property of atmospheric flow.''

Nevertheless, we begin by noting that as an initially gravitationally and symmetrically stable baroclinic atmosphere is destabilized by, for example, surface heating or increasing the vertical shear of the geostrophic wind, CSI/PSI will arise before CI/PI (Emanuel 1994, p. 410), but owing to the larger growth rate and energy release of moist gravitational convection compared to slantwise convection, gravitational convection, if initiated, is likely to dominate in time (Bennetts and Sharp 1982, pp. 598–599). Following Emanuel (1980, pp. 220, 245–250), Jascourt et al. (1988, pp. 188–189) term the situation where CI/PI and CSI/PSI coexist *convective–symmetric instability*. Therefore, the question arises as to the mesoscale circulations in the atmosphere to organize any resulting convection in such an environment.

Xu (1986a, p. 331) proposes two mechanisms for rainband development, mechanisms we now recognize as forms of convective–symmetric instability. The first he refers to as ''upscale development,'' where small-scale moist gravitational convection develops first, followed by mesoscale banded organization of clouds due to the release of symmetric instability as the environment becomes gravitationally stabilized. It seems that this type of development would be most likely to occur outside of frontal regions where small-scale moist gravitational convection organizes in the absence of synoptic-scale airmass boundaries. In contrast, Xu (1986a) refers to ''downscale development,'' where bands generated during frontal ascent in a moist symmetrically unstable environment lead to latent-heat release, effectively destabilizing the midtroposphere to gravitational convection. Eventually, the release of moist gravitational instability leads to band formation. Xu's (1986a) downscale development is similar to the three-stage process of frontal-precipitation-band development hypothesized by Bennetts and Hoskins (1979, 961–962).

A likely observational example of upscale development in a situation of convective–symmetric instability is documented by Jascourt et al. (1988). From a region of scattered cumulus over northern Louisiana, five parallel cloud bands simultaneously grew to become lines of thunderstorms. The bands were aligned along the 700–500-mb shear, a layer in which the moist symmetric stability was especially weak. The vertical stratification in the lower troposphere, however, was conditionally unstable to gravitational convection with CAPE of more than 1000 J kg^{-1}. Jascourt et al. (1988) hypothesize that the initial latent-heat release by the scattered cumulus in the layer of weak symmetric stability favored the development of convective–symmetric instability and organized the convection into the five bands. This case suggests that the nature and organization of convection can be modulated by the symmetric stability.

An alternate scenario for the release of upscale convective–symmetric instability is modeled by Zhang and Cho (1992), Seman (1994), and Bélair et al. (1995). Zhang and Cho (1992) and Bélair et al. (1995) use mesoscale numerical-model simulations of real squall lines to demonstrate how the typical structure of a squall line [a schematic of which is presented in Houze et al. (1989, Fig. 1)] acts to release both PI and PSI simultaneously, illustrated schematically in Fig. 5a, adapted from Seman (1991, 1992). The convective line reduces the moist gravitational instability, whereas remnant negative MPV_g is transported back toward the trailing precipitation region, where the release of PSI in the ascending front-to-rear flow helps to enhance precipitation (Fig. 5a). Despite the potentially large impact that the convective parameterization scheme may have in these studies (e.g., Molinari and Dudek 1992), these simulations appear to be consistent with the observation that

[5] Shields et al. (1991, p. 951, Figs. 15b and 17b) and Rauber et al. (1994, p. 197) also misuse the term CI when what was shown was PI (see section 3b).

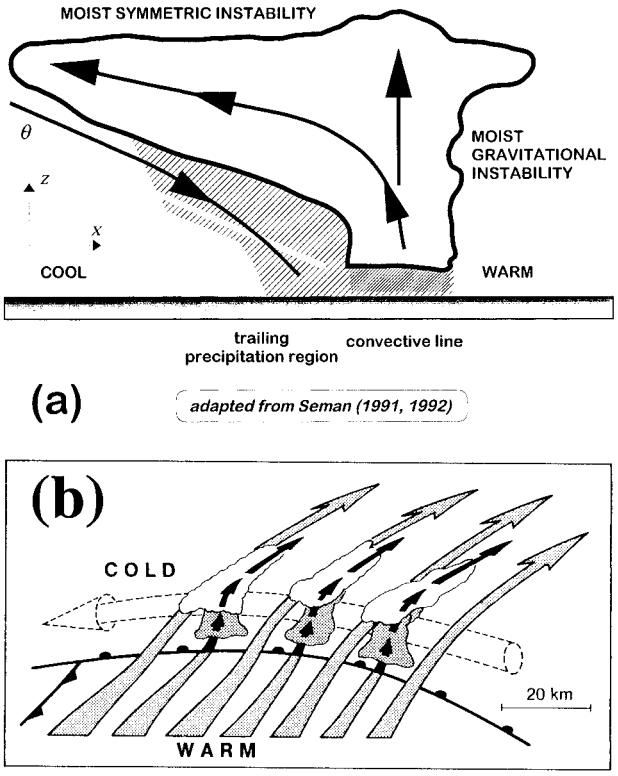

FIG. 5. (a) Schematic cross section of upscale convective–symmetric instability in a midlatitude mesoscale convective system [adapted from Seman (1991, 1992)]. Thick solid line encloses cloud (shaded). Thin solid lines with arrows represents direction of circulation. Gray solid line labeled θ represents orientation of typical potential-temperature contour in the cool air. Hatching is proportional to precipitation intensity. Moist gravitational instability is released within the convective line, remaining moist symmetric instability is released within the trailing precipitation region; dry-adiabatic descent initially occurs within rear inflow, which may become saturated due to precipitation evaporating/sublimating into the descending air. (b) Schematic of downscale convective–symmetric instability as depicted in the ''escalator–elevator'' warm-frontal-ascent model (Neiman et al. 1993, Fig. 8). Warm southerly airstream (flat, lightly stippled arrows) rises over the cold easterly polar airstream (tubular dashed arrow). Mesoconvective ascent (the elevator, solid arrows) and convective clouds (stippled with white anvils) are shown at regular intervals between regions of gentler ascent (the escalator).

the convective line is often characterized by lapse rates that are moist absolutely unstable (Fritsch and Bryan 1998), such that MPV_g^* is less than zero. These results are, in turn, consistent with those of Seman (1994), who shows that convection in an idealized environment similar to that of Jascourt et al. (1988) results in nearly upright updrafts. Slantwise ascent then occurs, releasing symmetric instability, followed by downdrafts that descend following sloping (dry and/or moist) isentropes (Fig. 5a). Comparison to a barotropic simulation (PI present only) indicates that the baroclinicity enhances the mesoscale circulation leading to more intense, longer-lived updrafts and more precipitation, consistent with the results of Xu (1986a). Case studies of upscale development in the presence of convective–symmetric instability and inertial instability are also presented by Blanchard et al. (1998).

Whether the trailing precipitation region behind a mesoscale convective system, oftentimes referred to as the stratiform region, is characterized by stratiform or convective precipitation is being debated.[6] The results of Zhang and Cho (1992) and Bélair et al. (1995), if general to mesoscale convective systems, would indicate that this region is characterized by slantwise convection due to the release of MSI. Indeed, further observational and modeling studies continue to suggest regions of MSI in the trailing precipitation region of squall lines (e.g., Jiang and Raymond 1995; Braun and Houze 1996). Therefore, referring to this region as ''stratiform'' (i.e., occurring in a stable environment) may have to be reconsidered.

Observed inhomogeneities in vertical motion and precipitation rate along frontal zones in the form of embedded bands or cells may suggest manifestations of downscale convective–symmetric instability. As the amount of moisture available to the circulation increases, the likelihood of generating embedded moist gravitational convection increases (Saitoh and Tanaka 1988). In a frontal environment initially characterized by PSI, Bennetts et al. (1988, 368–369) and Locatelli et al. (1994, Fig. 13) argue that the circulation associated with an embedded band will overturn contours of θ_e, thereby leading to PI, a result replicated in idealized models by Saitoh and Tanaka (1987), Innocentini and dos Santos Caetano Neto (1992), and Persson and Warner (1995). On the other hand, observational (Thorpe and Clough 1991) and modeling (Holt and Thorpe 1991; Dudhia 1993; Fischer and Lalaurette 1995a; Persson and Warner 1995) research shows that M_g surfaces can buckle, as well. But, as noted by Fischer and Lalaurette (1995b, p. 1318), experimental distinction between these two processes is difficult and indistinguishable in their final states, so the difference is probably academic.

A possible example of downscale convective–symmetric instability is Neiman et al.'s (1993) elevator/escalator concept for warm-frontal ascent (Fig. 5b) in which isolated regions of strong sloping ascent (45° to the horizontal) 10 km wide (the ''elevator'') contrast with weaker regions of gentler slantwise ascent (10° to the horizontal) roughly 15 km wide (the ''escalator''). Reuter and Yau (1993, p. 378) determine that the warm-frontal environment that Neiman et al. (1993) analyze is characterized by both PI and PSI, suggesting that the release of PI may be occurring in the ''elevator'' convective elements, while the release of PSI may be occurring in the ''escalator'' slantwise regions. Parsons and Hobbs (1983, p. 2385), Bennetts and Ryder (1984,

[6] The terminology *stratiform precipitation* as it pertains to precipitation in the trailing region of mesoscale convective systems is discussed by C. Doswell and J. Krácmar (http://www.nssl.noaa.gov/~doswell/stratiform/Stratiform_WWW.html) and Houze (1997).

Fig. 16), Byrd (1989, p. 1127), and Colman (1990a, b) also observe similar convective structures embedded in slantwise ascent in an environment characterized by both PI and PSI. Rainband studies before the advent of MSI theory in the early 1980s (e.g., Browning et al. 1973) and the idealized modeling work of Xu (1989b, Figs. 16 and 18) also may indicate such a process. These precipitation structures may represent a form of downscale convective–symmetric instability, where both moist gravitational and moist slantwise convection occur in an environment characterized by both moist gravitational and moist symmetric instabilities. That these precipitation structures commonly are observed may suggest that convective–symmetric instability is not atypical, as demonstrated, for example, by the large number of soundings from central Alberta exhibiting both moist gravitational and moist symmetric instabilities (Reuter and Aktary 1995, Table 7).

b. Deep convection, hurricanes, and lightning

It is sometimes stated that the existence of deep cumulonimbus, large precipitation rates, strong downdrafts, or lightning (i.e., thunderstorms) precludes moist slantwise convection (e.g., Bennetts and Sharp 1982, 598–599). We argue below that insufficient evidence exists to make such claims.

As in moist gravitational convection, moist slantwise convection can result in vertically shallow or deep circulations, depending on the thickness of the unstable layer and the level of neutral buoyancy (also known as the equilibrium level). Therefore, it is possible for slantwise convection to develop deep circulations. For example, the outward slope of the upper eyewall of hurricanes (e.g., Marks et al. 1992, Fig. 12f; Black and Hallett 1998, Fig. 10) suggests the presence of slantwise convection (e.g., Emanuel 1989; Black et al. 1994; Mathur 1997).

As discussed previously (e.g., in reference to Fig. 5a), updrafts of slantwise convection will ascend nearly along the saturated moist adiabat, whereas downdrafts descend dry adiabatically, overcoming the resistance of the positive buoyancy and compensating for the ascent (e.g., Marécal and Lemaître 1995, p. 301). Therefore, processes that cool the descending air would accelerate development of the slantwise circulation. Since sublimation of snow is more efficient, in general, than evaporation of rain in lowering the air temperature (Clough and Franks 1991), strong mesoscale downdrafts are most likely created by sublimating snow. In some observational and modeling research, sublimation of snow into dry downdrafts, possibly also influenced by precipitation loading, has led to saturation and rigorous descent (e.g. Ramstrom 1990; Stensrud et al. 1991; Thorpe and Clough 1991, 929–930; Emanuel 1992; Marécal and Lemaître 1995; Parker and Thorpe 1995; Zhang and Cho 1995; Braun and Houze 1997), approaching 20 m s^{-1} in some situations (Black et al. 1994). Thus quite strong circulations can result from slantwise ascent/descent due to the inclusion of diabatic effects, although the relative frequency of these more impressive vertical motions remains relatively unknown.

In isolated thunderstorms, it is generally accepted that strong updrafts exceeding 5 m s^{-1} favor coexisting ice and water phases that appear to be required for the generation of lightning. This would appear to exclude slantwise convection as being associated with lightning, since most slantwise updrafts are assumed to be weaker (tens of cm s^{-1} to a few m s^{-1}), although direct observations are lacking. On the other hand, Williams (1991, p. 2512) notes that the mechanisms that lead to charge separation are, in principle, independent of the existence of moist gravitational instability, indicating the possibility that lightning could be associated with slantwise convection. We currently recognize three environments characterized by MSI in which lightning is observed to occur.

The first environment characterized by both MSI and lightning is the trailing precipitation region of mesoscale convective systems. As discussed in section 5a, numerical and observational evidence indicates the presence of MSI in the trailing precipitation region, consistent with the occurrence of slantwise convection. The evidence for lightning in this region is reviewed by MacGorman and Rust (1998, 275–277).

The second environment is that of wintertime convection. While some cases of wintertime convection apparently are associated with CI (e.g., Engholm et al. 1990) or with convective–symmetric instability (e.g., Holle and Watson 1996), Colman (1990b, 1991) and Freedman (1995) argue for the possible coexistence of slantwise convection and lightning. MacGorman and Rust (1998, p. 292) summarize their review of lightning in winter storms with, ''we are aware of no thorough scientific investigation of causal relationships between the electrical state of winter storms and their snowfall. Extensive tests to evaluate the proposed hypotheses concerning possible links between lightning and the mesoscale and synoptic-scale meteorology associated with winter storms have yet to be performed.''

Finally, lightning has been observed in the eyewall during the deepening phase of mature hurricanes, although rarely (e.g., Molinari et al. 1994, 1999). As discussed previously, the eyewall can be treated as symmetrically neutral and is generally free of lightning activity. Therefore, lightning in the eyewall may indicate an outbreak of buoyancy-driven updrafts and temporary disruption of symmetric neutrality, resulting in intensification of the hurricane (Molinari et al. 1994, 1999).

Perhaps noncoincidently, these three environments also tend to be characterized by the occurrence of higher-than-normal percentages of positive cloud-to-ground lightning. Although not the only mechanism posited for the occurrence of positive lightning, some believe that strong vertical wind shears horizontally separate the cores of differently signed charges, thereby exposing

positive charge aloft to the ground (e.g., Orville et al. 1988; MacGorman and Rust 1998, 275, 290). We suggest that these environments also may be associated with MSI. This hypothesis, however, has not been rigorously defended.

Williams (1991) notes that evaluating MSI in these cases can be difficult, particularly eliminating CI completely from consideration. Nevertheless, coupled with our incomplete understanding of the conditions under which cloud electrification occurs (Vonnegut 1994), we do not know enough at this time to state conclusively that the existence of deep cumulonimbus, large precipitation rates, or lightning precludes the existence of slantwise convection. In fact, some evidence suggests otherwise.

6. Nature of the banding

Perhaps the most operationally significant use of MSI is to assess the nature of the precipitation banding (orientation, spacing, number of bands, movement, etc.) that may occur. The goal in operational forecasting is to anticipate the occurrence and nature of the large gradients in precipitation that can result if these bands remain nearly stationary. MSI theory makes certain predictions about the size, shape, movement, orientation, wavelength, and the existence of single or multiple bands. Yet, few studies evaluate those parameters as a test of whether MSI may have been associated with their cases of banded clouds and precipitation. In that regard, characteristics of banded clouds and precipitation in order to be considered associated with MSI are enumerated below [adapted from Seltzer et al. (1985, p. 2208)].

1) The bands and their environment should be nearly two-dimensional (i.e., be nearly ''symmetric''). The more two-dimensional the bands and their environment are, the better symmetric-instability theory will apply.
2) The condition for MSI should be met in the region of the bands.
3) The bands should be aligned nearly along the thermal wind and should be strongest in the region of the instability. Bands can deviate from the direction of the thermal wind, however, by as much as 15° anticyclonically in idealized models (Busse and Chen 1981; Miller and Antar 1986; Jones and Thorpe 1992; Zhang and Cho 1995; Gu et al. 1998) or greater in observations (e.g., Byrd 1989, Fig. 8; Colman 1990b, Fig. 17).
4) The bands, if they are moving, should be moving with the environmental flow (i.e., bands are advected by the flow; they do not propagate relative to the environmental flow).
5) The spacing between the bands should be related to the depth of the unstable layer and the slope of the isentropes, as expressed in Emanuel (1979) and Seltzer et al. [1985, (3.3)].
6) The slope of the ascent in the region of the bands should lie between the slopes of moist adiabatic and M_g surfaces. When the flow is hydrostatic, the ascent will occur exactly on the isentropic surfaces.

In this section, we review previous work attributing banding of clouds and precipitation to MSI and evaluate their methodologies in search of useful methods to predict banding of clouds and precipitation. Previous observational studies of banded precipitation are summarized also by Lagouvardos et al. (1993, Table 1).

Seltzer et al. (1985) examine 15 banded and nonbanded precipitation events (as determined by Doppler radar) over New England and find substantial agreement between theory and their observations, indicating that MSI is likely associated with the banded precipitation in these events. The degree of banding appears to be strongly related to the magnitude of the maximum wind shear with better-defined banding more likely for shears exceeding 13 m s^{-1} km^{-1}. They also show that the band orientations are close to the 1000–500-mb thickness contours and the observed wavelengths agree well with the predicted values from theory for most cases. Problems with large ageostrophic shear and curvature, and assessing geostrophy from the sparse soundings in some of their cases, may have limited the success of their study.

Another limitation of Seltzer et al. (1985) is that the lifting mechanism is not identified, as they explicitly attempt to eliminate the effects of frontogenesis by requiring surface fronts and low pressure centers to be more than 500 km away from the region of analysis. Sanders (1986) notes a potential pitfall in this approach, however. Reanalyzing one of Seltzer et al.'s (1985) cases, Sanders (1986) finds that lower-tropospheric frontogenesis is likely occurring in the region of banded precipitation northwest of the surface low center, a condition that Seltzer et al. (1985) explicitly try to eliminate from their cases. Unfortunately, published studies of similar synoptic situations exist in which the authors do not calculate frontogenesis (e.g., Snook 1992; Reuter and Nguyen 1993). Consequently, these studies may be susceptible to the same pitfall, reiterating the importance of calculating forcing for ascent for individual cases in the vicinity of where MSI might be present. Therefore, since forcing for ascent need not be surface based, but can exist above the boundary layer, the absence of analyzed surface fronts is not adequate for eliminating the possibility of frontogenetical forcing for ascent.

Further examples of climatologies of banded clouds and precipitation include Bennetts and Hoskins (1979), Bennetts and Sharp (1982), and Byrd (1989). Bennetts and Hoskins (1979, section 5) examine 36 cases of satellite and radar data and do not find a strong relationship between Richardson number and banding. Bennetts and Sharp (1982, section 4) consider 30 cases of banded precipitation and 14 cases of nonbanded precipitation. They note that, for large values of the MSI growth-rate

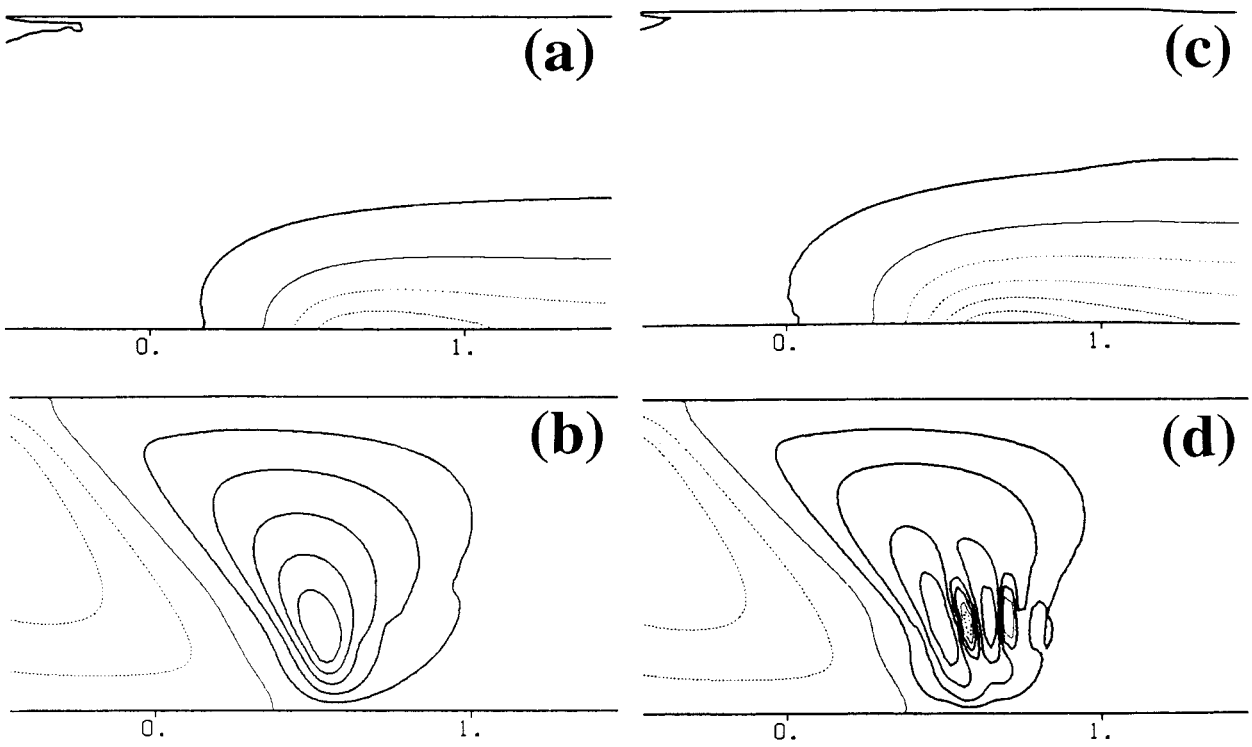

FIG. 6. (a) Case with localized frontogenetical forcing and small negative MPV_g: initial MPV_g (contoured every 0.5×10^{-12} s^{-4}; thick solid, thin solid, and dashed are used for positive, zero, and negative values, respectively). (b) Case with localized frontogenetical forcing and small negative MPV_g: vertical velocity at 16.7 h (drawn with power-increasing intervals $\pm 2^n \times 0.5$ cm s^{-1}; thick solid, thin solid, and dashed are used for positive, zero, and negative values, respectively). (c) and (d) The same as (a) and (b), respectively, except for case with localized frontogenetical forcing and large negative MPV_g. The horizontal scale in all panels (from 0.0 to 1.0) is 1000 km. Figures are from Xu's (1992, Figs. 1b, 2a, 4, and 6a) cases I and II.

parameter, the precipitation is likely to be banded, whereas for small positive values and negative values, the growth-rate parameter is not very useful in discriminating banded from nonbanded precipitation. Byrd (1989) finds similar results in 27 ''overrunning'' precipitation events (226 soundings) over the southern Plains. He notes that over 80% of his banded and strongly banded cases meet the Richardson-number criteria for MSI, but nearly 60% of the nonbanded cases do also, suggesting limited utility of this parameter for discrimination, in agreement with Bennetts and Sharp (1982). A complication is that his strongly banded category has higher incidences of PI (Byrd 1989, p. 1127), perhaps suggesting the occurrence of banded convection associated with the release of pure moist gravitational instability or convective–symmetric instability (section 5a). Byrd (1989, p. 1124) also noted stronger wind shear in the boundary layer for strongly banded events. This body of research suggests that well-constructed climatologies of even a small number of events [as suggested by DeVoir (1998)] may produce useful results, evaluating the likely existence of slantwise convection associated with MSI.

Whether single or multiple bands form in the presence of frontogenesis is addressed using idealized numerical models. As discussed in section 4, the results of Emanuel (1985) and Thorpe and Emanuel (1985) indicate that weak positive symmetric stability in the warm air in the presence of frontogenesis leads to a single band of ascent that narrows as the symmetric stability approaches neutrality. In general, the inviscid Sawyer–Eliassen equation cannot be solved when PV_g (or MPV_g, when moist) is negative. Adding viscous effects to the Sawyer–Eliassen equation (Xu 1989a), however, permits solutions when PV_g (or MPV_g, when moist) is negative. Therefore, using a viscous form of the Sawyer–Eliassen equation in the presence of localized frontogenetical forcing, Xu (1989b) finds a single band of ascent for positive symmetric stability. As the MPV_g is decreased toward zero and becomes negative, the single band becomes narrow and intense (Figs. 6a,b). If the forcing becomes horizontally widespread and MPV_g is negative, multiple bands become embedded within the larger-scale frontal circulation, consistent with Knight and Hobbs (1988, p. 926). If the forcing remains localized and MPV_g is decreased further, the multiple bands become more intense and more widely spaced (Figs. 6c,d). These idealized modeling experiments help to explain the observations of Bennetts and Sharp (1982) and Byrd (1989) that many nonbanded situations may exceed the

criteria for MSI. These experiments further suggest that a balance between the magnitude and areal extent of the frontogenetical forcing, the eddy viscosity, the moisture availability, and the value of the MPV_g exists that determines whether single or multiple bands form, but observational verification of these idealized–modeling experiments has not been forthcoming.

Based on the results of this observational and modeling work, it is clear that, in a forecasting mode, even if a region of the atmosphere meets the criteria for MSI, the formation of banded structures cannot be assumed a priori. On the other hand, the existence of banded structures, and the validation of the observed structures to those predicted by MSI theory, is strong evidence for the bands being associated with the release of MSI. The above results also indicate that, even in the presence of frontogenesis, multiple bands can form, although the conditions under which single versus multiple bands would form have not been validated in a rigorous way at this time. Therefore statements such as ''the [existence of] multiple bands . . . indicate[s] that CSI is a more likely candidate for the observed precipitation than frontogenetical forcing'' (Snook 1992, p. 438) are not accurate.

7. MSI in mesoscale-model simulations

The growth in availability of quality gridded atmospheric datasets (e.g., Keyser and Uccellini 1987) makes determination of MSI in those datasets relatively easy (e.g., Bennetts and Sharp 1982; Snook 1992; Grumm and Nicosia 1997; Martin 1998; Wiesmueller and Zubrick 1998). A reasonable question is whether MSI and its attendant circulations can be assessed accurately in these datasets. Crucial tests of the effect of horizontal and vertical resolution on unforced (no frontogenesis, radiative, or surface forcing acting on the MSI, i.e., no externally applied lifting mechanism), hydrostatic, nonlinear MSI in a mesoscale model are performed by Persson and Warner (1991, 1993) and Ducrocq (1993). They find that horizontal/vertical grid spacings greater than 30 km/0.34 km are inadequate to resolve the resulting circulations explicitly. To capture the most unstable mode, grid spacings no greater than 15 km/0.17 km are required. If the most unstable mode is not adequately resolved, then the resulting evolution of the MSI circulations is substantially slower and the amplitude reduced from what would be expected in the real atmosphere. Even in the presence of lower-tropospheric frontogenesis, these results are consistent with those of Knight and Hobbs (1988), who find that hydrostatic nonlinear MSI bands are absent at 80-km horizontal grid spacing, poorly resolved at 40 km, and well-resolved at grid spacings of 5–10 km.

In comparison, observations of banded structures indicate typical widths of the bands of 20–100 km (e.g., Byrd 1989) and typical distances between bands of 10–220 km, (e.g., Seltzer et al. 1985; Byrd 1989; Lagouvardos et al. 1993). Therefore, consider a mesoscale model with horizontal resolution of 20–90 km, values typical of the short-range operational forecast models at the National Centers for Environmental Prediction, simulating convection over a region with MSI. In this scenario, the model may be able to resolve the larger-scale frontogenetical circulation, if present, but not the smaller-scale bands.

Inadequate model resolution prohibits explicit resolution of the scales responsible for banded precipitation. Besides the underprediction of maximum vertical velocities, a less vigorous circulation in the model would decrease the region of saturation, decreasing the likelihood of releasing heretofore untapped regions of MSI. Therefore, modeled precipitation rates would be substantially less than those observed, despite perhaps a reasonably accurate simulation of the precipitating region. An example of this situation is presented in Martin (1998, p. 333, Fig. 6), who observes two 35-km-wide snowbands on radar, separated by 35 km and parallel to the thermal wind, suggestive of the presence of MSI. Martin (1998) examines the potential for the release of MSI in a mesoscale-model simulation of this event and finds that the necessary conditions for instability and lift are present, but inadequate moisture exists to reach saturation. Hence, he concludes that, based on the model simulation, MSI could not have been responsible for the observed snowbands. His analysis, however, employs a mesoscale model with 40-km horizontal grid spacing. Although the model is too coarse to resolve the observed snowbands, Martin (1998, p. 335) states that he desires an accurate simulation of the narrow region of snowfall, rather than an accurate simulation of the individual snowbands comprising the event. Consequently, the coarse resolution of the model results in the areal extent of the precipitation being reasonably well forecast, but the magnitude of the precipitation maxima are underforecast by as much as 50% (Martin 1998, cf. Figs. 1 and 4). Although many explanations may be proposed for the underprediction of the precipitation maxima, Knight and Hobbs (1988), Ducrocq (1993), and Persson and Warner (1991, 1993) show that the model resolution has a large impact on the ability to simulate MSI circulations properly, results consistent with those of Martin (1998).

Molinari and Dudek (1992, section 5) discuss the implications for slantwise convection in numerical weather prediction models. Whereas grid-resolvable precipitation is calculated by the large-scale explicit precipitation schemes, convective precipitation due to the release of moist gravitational instability is calculated by cumulus parameterization schemes. Precipitation generated by the release of MSI during slantwise convection, however, is neither grid-resolvable nor convectively parameterized at resolutions greater than about 10 km. The inclusion of this missing effect may substantially improve the numerical prediction of quantitative precipitation, as suggested by Emanuel (1983a, p. 2375) and

Persson and Warner (1993, p. 1832). Balasubramanian and Yau (1995) apply a parameterization for slantwise convection for an idealized three-layer model of cyclogenesis in which they illustrate the importance of the release of MSI along the warm and back-bent warm fronts, which aids in deepening the surface cyclone. Their results are in agreement with those of Cao and Cho (1995), who found that negative MPV is generated first in the warm sector near the north end of the cold frontal zone, then develops along the bent-back front at the mature stage. For a simulation of a central United States cyclone, Lindstrom and Nordeng (1992) apply Nordeng's (1987, 1993) parameterization of slantwise convection patterned after the Kuo scheme for moist gravitational convection, which produces neutrality to slantwise convection along a M surface. Their results (Fig. 7) show that the parameterization improves the simulation of the quantity and areal extent of precipitation associated with a midwest United States cyclone, indicating the potential usefulness of this approach. Also, the addition of the slantwise-convective parameterization helps the model generate divergent circulations more quickly (improving the so-called model-spinup problem). Although Molinari and Dudek (1992, section 5) suggest that slantwise convection could occur on the grid scale in models, they also caution that their conclusions are based on limited research results, which do not include the contemporaneous research of Lindstrom and Nordeng (1992). Consequently, future research in this area might result in improvements in quantitative precipitation forecasting. Whereas operational implementation of slantwise-convective parameterization in research-mesoscale and operational-forecast models is less imperative with the push to smaller horizontal grid spacing, the climate-modeling community will have need to deal with slantwise convection for the foreseeable future.

An additional concern for assessing MSI using mesoscale-model output involves how the model is initialized. Observations of water substance (vapor, cloud water, hydrometeors) in the atmosphere tend to be more sparse than observations of the thermal, wind, or mass fields. Therefore, models rely heavily on developing their own water fields. If the model simulation is started as a static initialization (i.e., lacks cloud water and precipitation fields at the initial time; the so-called cold start), like many real-time (Mass and Kuo 1998, Table 1) and research mesoscale models, then it will take time for the model to spin up and generate those fields. Depending on the synoptic situation and model resolution, estimates of the typical time for model spinup to occur range from 1–12 h. The model-spinup dilemma may pose a problem for the interpretation of Martin's (1998) results, as the time at which the assessment of MSI occurs (0600 UTC 19 January 1995) is only 6 h after model initialization time, comparable to the model spinup time. This is possibly an inadequate amount of time to have fully developed cloud and precipitation fields. Therefore, it is likely that the relative humidity fields may underestimate the saturated area, which in turn would underestimate the area susceptible to slantwise convection. This may be another factor that contributes to the underestimate of the modeled precipitation (Martin 1998, cf. Figs. 1 and 4). On the other hand, the National Centers for Environmental Prediction operational forecast models are run in a continuous assimilation cycle, which limits this spinup problem.

A final point is that different numerical models reach saturation and generate clouds at different relative humidities [an approach described by Mathur (1983) and Mocko and Cotton (1995)]. For example, in the version of the Eta model (as of November 1998), clouds begin to develop at relative humidities of 95% over the ocean surface, ramping down to 80% over the lowest 10 model levels, and 75% over land (G. DiMego, Q. Zhao, and E. Rogers 1998, personal communication; Zhao et al. 1997, p. 699), 80% in the Nested Grid Model (NGM; Hoke et al. 1989, p. 331), but 100% in the Rapid Update Cycle (RUC; S. Benjamin 1998, personal communication). It is also of import that gridpoint values of relative humidity in the Eta model rarely exceed 95% (G. DiMego and E. Rogers 1998, personal communication). Knowing these critical values is essential to assessing whether slantwise convection may be present within mesoscale-model data. Proper use of model data for assessing slantwise convection, especially early in the simulation when model spinup may be important, mandates knowledge of the model characteristics. If model output is used wisely, then we believe it can be useful.

Thus, operational implementation of MSI techniques in the forecast office tends to consist of the following methodology (Grumm and Nicosia 1997, 21–22; Wiesmueller and Zubrick 1998, section 7). First, an evaluation of the model output for areas meeting the MSI criteria over a large area for up to 2 days in advance is performed. If a particular area is susceptible to MSI, then that area is monitored into the short-range period (0–12 h). Since the model resolution is too coarse to resolve individual precipitation bands, the forecaster then must rely more heavily on the observations at this stage. Bands, if they form, can be monitored for locally heavy precipitation amounts and short-term forecasts can be issued. At this time, there does not appear a way to be more specific about the location of bands before they form, akin to the difficulty in forecasting individual thunderstorms prior to initiation.

8. Concluding summary

In conclusion, we first summarize our principal conclusions and recommendations in section 8a, followed by directions for future research in section 8b. This article concludes with thoughts about the use of CSI (symbols and acronyms are defined in the appendix) in research and operational forecasting practice in section 8c.

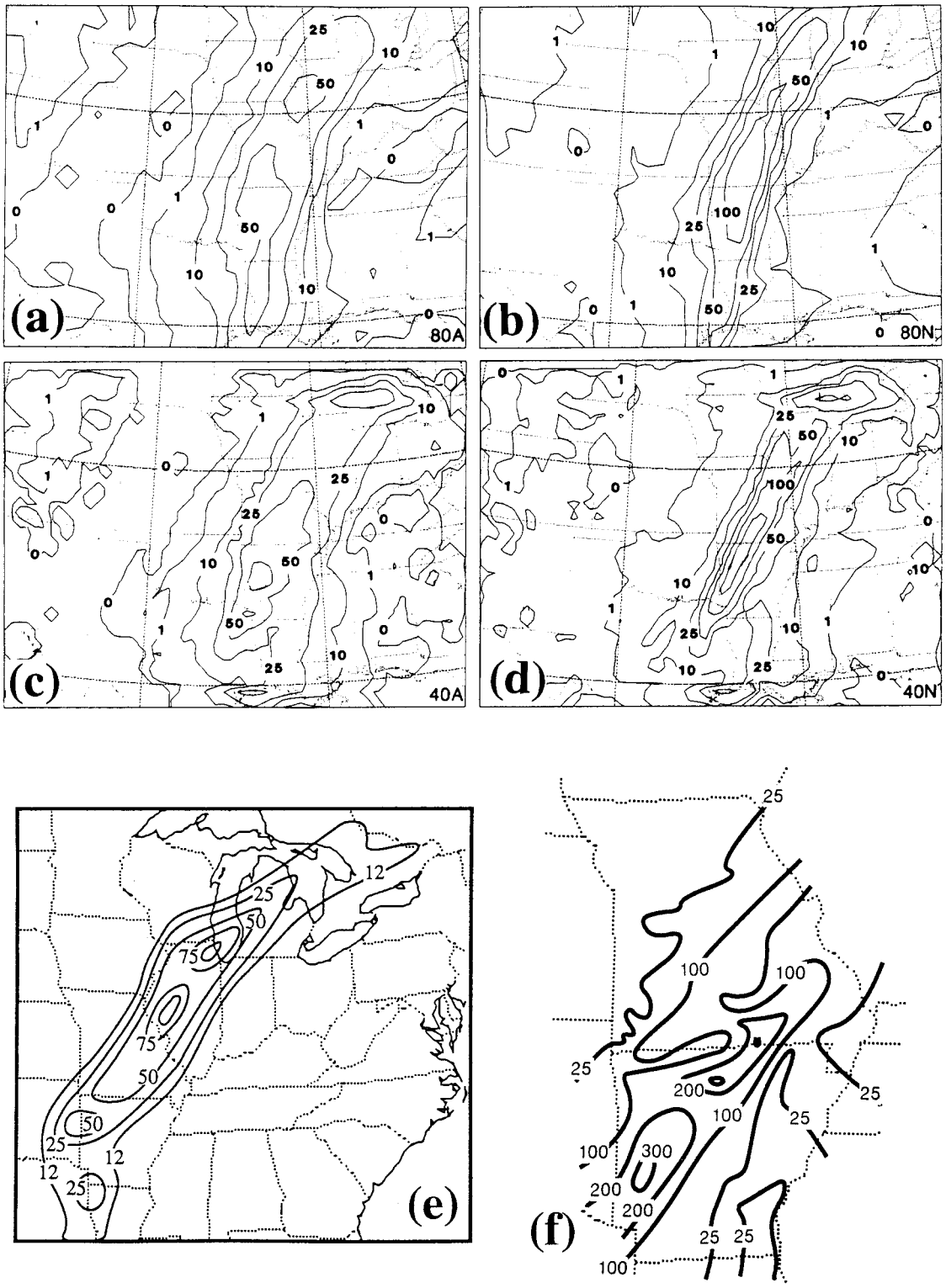

FIG. 7. Total accumulated 24-h precipitation from simulations [(a) and (b)] with 80-km horizontal grid spacing and [(c) and (d)] 40-km horizontal grid spacing with [(a) and (c)] Anthes–Kuo convective parameterization and [(b) and (d)] with both Anthes–Kuo and Nordeng convective and slantwise parameterizations. Contour values of 0, 1, 10, 25, 50, 100, and 200 mm shown. (e) Synoptic-scale analysis of 24-h rainfall ending 1200 UTC 3 Dec 1982. Contour values of 12, 25, 50, 75, and 100 mm. (f) Analysis of 24-h rainfall ending 1200 UTC 3 Dec 1982 in Arkansas and Missouri. Contour values of 25, 100, 200, and 300 mm. Figures from Lindstrom and Nordeng (1992, Figs. 8, 1, and 2, respectively).

a. Principal conclusions and recommendations

The following points represent our basic tenets regarding MSI discussed in this article.

1) Like deep, moist gravitational convection, moist slantwise convection requires the simultaneous presence of instability, moisture, and lift. The absence of any one of these three is sufficient to prevent moist slantwise convection from occurring (section 2).
2) The terms CSI and slantwise convection do not have interchangeable meanings (section 2).
3) Strictly, hydrostatically and geostrophically balanced basic states for $\overline{\theta}_e^*$ and M_g, respectively, are required for determination of CSI. In practice, the restriction on $\overline{\theta}_e^*$ can be relaxed to θ_e^*, but M_g should not be relaxed to M (sections 3a and 3b).
4) Analogies to CI and PI indicate that the definitions commonly employed for CSI are really for PSI. Ideally, when assessing CSI, θ_e^* should be used; when assessing PSI, θ_e should be used (section 3b).
5) Owing to the potential confounds with assessing the M_g–θ_e^* relationship, we recommend that MPV_g^* or another measure of CSI not dependent on cross-section orientation (e.g., SCAPE), along with a measure of CI and inertial instability, be employed to assess CSI (sections 3c and 5).
6) Even if the atmosphere is determined to be stable to moist slantwise and moist gravitational convection, banded clouds and precipitation may still form owing to forced ascent (section 3f).
7) By definition, an environment characterized by CSI possesses a horizontal gradient in θ_e^* and vertical wind shear, likely indicating a frontal zone. In an environment in which CSI and frontogenesis coexist, it is improper to attempt to separate the circulations due to CSI from the frontal circulation (section 4).
8) Blindly applying tests for CSI/PSI may result in the identification of regions of CI/PI or inertial instability (section 5).
9) The coexistence of CSI/PSI and CI/PI, as well as adequate moisture and lift, may result in a mixture of moist gravitational and moist slantwise convection associated with the release of convective–symmetric instability (section 5a).
10) The existence of deep cumulonimbus, large precipitation rates, strong downdrafts, or lightning is not an adequate discriminator between the existence of moist gravitational and moist slantwise convection (section 5b).
11) The nature of banding in clouds or precipitation appears to be only weakly related to measures of CSI. More attention should be paid, however, to evaluating other parameters (band spacing, movement, orientation, etc.) associated with bands suspected of being related to CSI (section 6).
12) The resolution of most research mesoscale and operational forecast models is inadequate to resolve individual CSI circulations. Consequently, care should be taken in assessing model data for CSI (section 7).

b. Future research

The preceding sections have presented an overview of the current knowledge and perspectives on CSI and slantwise convection. Observational, idealized model, and mesoscale-model studies have contributed to our present understanding. Despite the progress, a number of unresolved problems and issues can be identified and serve as subjects for further consideration. Among the topics that require further research are 1) assessing MSI, 2) nature of banding, 3) slantwise-convective parameterization, and 4) convective–symmetric instability and the general nature of atmospheric convection.

As illustrated in this review (particularly, section 3b), the specific diagnostics used to assess MSI are often misused. In particular, the choice of a particular thermodynamic quantity (θ_e or θ_e^* as measures of PSI or CSI, respectively) can affect the assessment of instability. The relative advantages and disadvantages of diagnosing PSI versus CSI have not been explored. Although we have suggested using CSI rather than PSI, case studies illustrating the structure and evolution of these fields prior to convective initiation have not been examined in general. For example, it is observed that moist gravitational convection can be manifest in a variety of ways that include supercell thunderstorms, mesoscale convective complexes, squall lines, and pulse (''airmass'') thunderstorms. Perhaps this sort of variety with slantwise convection is waiting to be explored. If that were the case, then it may be that certain diagnostics would work better for given situations in assessing various manifestations of slantwise convection. As an example, we have suggested in section 4 that SCAPE may be more useful to forecasting activated slantwise convection than statistical-equilibrium slantwise convection, but this hypothesis has not been tested operationally. Consequently, the relative merits of these diagnostics remain untested and awaits further research.[7]

Section 6 discussed the nature of banding from both an observational and idealized-modeling perspective. Unfortunately, studies that bridge the gaps between these two perspectives have not been performed. For example, a variety of idealized-modeling experiments of both forced and unforced MSI (e.g., Xu 1986a, 1989b, 1992; Zhang and Cho 1995; Arbogast and Joly 1998) suggest that a useful relationship might exist for forecasting the nature of the banding as a function of frontogenetical forcing, friction, moisture availability,

[7] Various diagnostic approaches for assessing slantwise convection are shared at our web site: http://www.nssl.noaa.gov/~schultz/csi.

and stability, yet there have been no rigorous observational or idealized-modeling attempts to validate this hypothesis. Also, as noted by Jones and Thorpe (1992, p. 257), idealized-modeling studies incorporating three-dimensional basic states have not been adequately explored. Also, Zhang and Cho (1995, 59–60) discuss the importance of three-dimensional simulations for obtaining more realistic banded precipitation. Toward this goal, Gu et al. (1998) have found that two-dimensional nonlinear symmetric circulations can be unstable in three dimensions and they resemble some observed three-dimensional substructures embedded in frontal rainbands.

As discussed in section 7, the addition of slantwise-convective parameterizations to mesoscale numerical models dramatically improved the forecast of the intensity and areal extent of precipitation, in at least one case (Lindstrom and Nordeng 1992). Consequently, slantwise-convective parameterizations should be developed, tested, and, if found to be useful, implemented in research mesoscale, operational forecast, and general circulation models with the aim of improving the prediction of quantitative precipitation (section 7).

The concept of convective–symmetric instability (section 5a) has not been examined in detail in the previous literature, and, as a result, there is much to be learned about convective–symmetric instability from both observational and idealized-modeling perspectives. Given the typical inhomogeneous condition of the atmosphere, areas favorable for MSI may be juxtaposed with areas favorable for gravitational convection (e.g., Fig. 4) such that convection can possess characteristics of slantwise convection, gravitational convection, or both, and may evolve from one form to the other. Consequently, convection can manifest itself in a variety of ways, depending on the environmental stability, lift mechanism, amount of moisture, and other factors. Overlaying radar and lightning data with MSI diagnostics can provide information about storm structure and evolution. The deficiency in our knowledge of this area is reiterated by Mapes (1997, p. 355), who states that the role of mesoscale organization in determining the amount (and nature) of the convection remains unclear. In addition, Jones and Thorpe (1992, 251–252, 257) state that three-dimensional effects appear to increase the susceptibility of symmetric instability to PI, leading to small-scale structure along the length of the bands. The issue of whether ''horizontal convection'' caused by the release of inertial instability plays a role also has been inadequately addressed. The work of Seman (1994) and Blanchard et al. (1998) suggests several ways that the atmosphere responds to situations where two or more instabilities are present. These issues may force rethinking the nature of convection beyond compartmentalizing atmospheric motions into either gravitational, slantwise, or horizontal convections (e.g. Xu and Clark 1985).

c. Conclusions

Within this article, previous literature on MSI and slantwise convection is reviewed. Drawing parallels to the familiar conceptualizations of gravitational convection allows a reconsideration of the extent to which slantwise convection is understood and used in research and forecasting environments. Indeed, the argument could be made that the near omnipresence of baroclinicity in midlatitudes, even during the warm season, requires an evaluation of the potential for slantwise convection. An example where such diagnosis might be useful is during the early and late stages of deep, moist convection, when gravitational instability is likely to be small. The dichotomy between gravitational and slantwise convection is also apparent in numerical modeling where parameterizations for slantwise convection presently are not included in the majority of research-mesoscale and operational-forecast models. Consideration of convective–symmetric instability appears to be a prudent step toward a more general consideration of atmospheric convection. It is tempting to speculate that combining the intellectual resources of those studying meso- and synoptic-scale processes with those studying convective-scale phenomena, from both the research and operational communities, has the potential to lead to further improvements in our understanding of convective phenomena.

Acknowledgments. We have benefited considerably from the advice and comments of Michael Baldwin, Steven Corfidi, Greg DeVoir, Paul Janish, Ann McCarthy, and Drs. Daniel Keyser, Donald MacGorman, John Molinari, James Moore, Richard Rotunno, David Rust, Terry Schuur, Charles Seman, Alan Thorpe, and Jeff Trapp. Insightful reviews of earlier versions of this manuscript were provided by George Bryan, Ronald Holle, and Drs. David Blanchard, Kerry Emanuel, Jack Kain, Robert Maddox, Jonathan Martin, John Nielsen-Gammon, Paul Roebber, David Stensrud, Robert Weisman, Earle Williams, and Qin Xu. Katherine Day (NOAA Library, Boulder, Colorado) obtained lists of references at our request, assuring a thorough bibliography to draw upon for this review. The first author thanks Dr. Charles Doswell III for his invaluable discussions/arguments on atmospheric convection and encouragement during the preparation of this manuscript. Most of this research was conducted while the first author was a National Research Council Postdoctoral Research Associate at the National Severe Storms Laboratory. This work is inspired by and dedicated to the late Dr. Bernard Vonnegut, who challenged us to scrutinize paradigms.

APPENDIX

List of Symbols and Acronyms

CAPE	Convective available potential energy
CI	Conditional instability

c_p	Specific heat of dry air at constant pressure
CSI	Conditional symmetric instability
f	Coriolis parameter
g	Gravity; subscript denoting geostrophic
gr	Subscript denoting gradient
L	Latent heat of vaporization
LFSC	Level of free slantwise convection
M	Absolute momentum defined as $v + fx$
M_g	Geostrophic absolute momentum defined as $v_g + fx$
MPV	Moist potential vorticity defined as $g\eta \cdot \nabla\theta_e$
MPV_g	Moist geostrophic potential vorticity defined as $g\eta_g \cdot \nabla\theta_e$
MPV_g^*	Saturated geostrophic potential vorticity defined as $g\eta_g \cdot \nabla\theta_e^*$
MSI	Moist symmetric instability
NGM	Nested Grid Model
PI	Potential instability (also called convective instability)
PSI	Potential symmetric instability
PV	Potential vorticity defined as $g\eta \cdot \nabla\theta$
PV_g	Geostrophic potential vorticity defined as $g\eta_g \cdot \nabla\theta$
q_{vs}	Saturation mixing ratio
RUC	Rapid Update Cycle
r	Distance along radius of curvature
SCAPE	Slantwise convective available potential energy
T	Temperature
v	Component of wind in alongfront direction
v_g	Component of geostrophic wind in alongfront direction
v_{gr}	Component of gradient wind in alongfront direction
x	Cross-front coordinate
z	Height coordinate
Γ_d	Dry-adiabatic lapse rate
Γ_m	Moist-adiabatic lapse rate
ζ_g	Vertical component of geostrophic relative vorticity vector
η	Three-dimensional absolute vorticity vector
η_g	Three-dimensional geostrophic absolute vorticity vector
θ	Potential temperature
θ_e	Equivalent potential temperature
θ_e^*, θ_{es}	Saturated equivalent potential temperature
θ_w	Wet-bulb potential temperature
∇	Gradient operator in x, y, and z coordinates
$\overline{( )}$	Basic state

REFERENCES

Arbogast, P., and A. Joly, 1998: Potential vorticity inversion of a two-dimensional steady flow: Application to symmetric instability. *Quart. J. Roy. Meteor. Soc.,* **124,** 317–339.

Balasubramanian, G., and M. K. Yau, 1995: Explosive marine cyclogenesis in a three-layer model with a representation of slantwise convection: A sensitivity study. *J. Atmos. Sci.,* **52,** 533–550.

Barnes, S. L., F. Caracena, and A. Marroquin, 1996: Extracting synoptic-scale diagnostic information from mesoscale models: The Eta model, gravity waves, and quasigeostrophic diagnostics. *Bull. Amer. Meteor. Soc.,* **77,** 519–528.

Bélair, S., D.-L. Zhang, and J. Mailhot, 1995: Numerical prediction of an intense convective system associated with the July 1987 Montreal flood. Part II: A trailing stratiform rainband. *Atmos.–Ocean,* **33,** 475–500.

Bennetts, D. A., and B. J. Hoskins, 1979: Conditional symmetric instability—A possible explanation for frontal rainbands. *Quart. J. Roy. Meteor. Soc.,* **105,** 945–962.

——, and J. C. Sharp, 1982: The relevance of conditional symmetric instability to the prediction of mesoscale frontal rainbands. *Quart. J. Roy. Meteor. Soc.,* **108,** 595–602.

——, and P. Ryder, 1984: A study of mesoscale convective bands behind cold fronts. Part I: Mesoscale organization. *Quart. J. Roy. Meteor. Soc.,* **110,** 121–145.

——, J. R. Grant, and E. McCallum, 1988: An introductory review of fronts. Part I: Theory and observations. *Meteor. Mag.,* **117,** 357–370.

Black, R. A., and J. Hallett, 1998: The mystery of cloud electrification. *Amer. Sci.,* **86,** 526–534.

——, H. B. Bluestein, and M. L. Black, 1994: Unusually strong vertical motions in a Caribbean hurricane. *Mon. Wea. Rev.,* **122,** 2722–2739.

Blanchard, D. O., W. R. Cotton, and J. M. Brown, 1998: Mesoscale circulation growth under conditions of weak inertial instability. *Mon. Wea. Rev.,* **126,** 118–140.

Bluestein, H. B., 1986: Fronts and jet streaks: A theoretical perspective. *Mesoscale Meteorology and Forecasting,* P. S. Ray, Ed., Amer. Meteor. Soc., 173–215.

——, 1993: *Synoptic-Dynamic Meteorology in Midlatitudes.* Vol. 2, *Observations and Theory of Weather Systems.* Oxford University Press, 594 pp.

Braun, S. A., and R. A. Houze Jr., 1996: The heat budget of a midlatitude squall line and implications for potential vorticity production. *J. Atmos. Sci.,* **53,** 1217–1240.

——, and ——, 1997: The evolution of the 10–11 June 1985 PRESTORM squall line: Initiation, development of rear inflow, and dissipation. *Mon. Wea. Rev.,* **125,** 478–504.

Browning, K. A., M. E. Hardman, T. W. Harrold, and C. W. Pardoe, 1973: The structure of rainbands within a mid-latitude depression. *Quart. J. Roy. Meteor. Soc.,* **99,** 215–231.

Busse, F. H., and W. L. Chen, 1981: On the (nearly) symmetric instability. *J. Atmos. Sci.,* **38,** 877–880.

Byrd, G. P., 1989: A composite analysis of winter season overrunning precipitation bands over the Southern Plains of the United States. *J. Atmos. Sci.,* **46,** 1119–1132.

Cao, Z., and H.-R. Cho, 1995: Generation of moist potential vorticity in extratropical cyclones. *J. Atmos. Sci.,* **52,** 3263–3281.

Chan, D. S. T., and H.-R. Cho, 1989: Meso-β-scale potential vorticity anomalies and rainbands. Part I: Adiabatic dynamics of potential vorticity anomalies. *J. Atmos. Sci.,* **46,** 1713–1723.

Chen, C., W.-K. Tao, P.-L. Lin, G. S. Lai, S.-F. Tseng, and T.-C. C. Wang, 1998: The intensification of the low-level jet during the development of mesoscale convective systems on a mei-yu front. *Mon. Wea. Rev.,* **126,** 349–371.

Cho, H.-R., and D. Chan, 1991: Meso-β scale potential vorticity anomalies and rainbands. Part II: Moist model simulations. *J. Atmos. Sci.,* **48,** 331–341.

Clough, S. A., and R. A. A. Franks, 1991: The evaporation of frontal and other stratiform precipitation. *Quart. J. Roy. Meteor. Soc.,* **117,** 1057–1080.

Colman, B. R., 1990a: Thunderstorms above frontal surfaces in environments without positive CAPE. Part I: A climatology. *Mon. Wea. Rev.,* **118,** 1103–1121.

——, 1990b: Thunderstorms above frontal surfaces in environments without positive CAPE. Part II: Organization and instability mechanisms. *Mon. Wea. Rev.,* **118,** 1123–1144.

——, 1991: Reply. *Mon. Wea. Rev.,* **119,** 2514–2515.

Davidson, N. E., K. Kurihara, T. Kato, G. Mills, and K. Puri, 1998: Dynamics and prediction of a mesoscale extreme rain event in the Baiu Front over Kyushu, Japan. *Mon. Wea. Rev.,* **126,** 1608–1629.

DeVoir, G. A., 1998: Conditional symmetric instability—Methods of operational diagnosis and case study of 23–24 February 1994 eastern Washington/Oregon snowstorm. National Weather Service Western Region Tech. Memo. 254, 16 pp. [Available from http://www.wrh.noaa.gov/wrhq/CSITM/webtm.htm.]

Donaldson, N. R., and R. E. Stewart, 1989: On the precipitation regions within two storms affecting Atlantic Canada. *Atmos.–Ocean*, **27,** 108–129.

Doswell, C. A., III, 1987: The distinction between large-scale and mesoscale contribution to severe convection: A case study example. *Wea. Forecasting,* **2,** 3–16.

——, and E. N. Rasmussen, 1994: The effect of neglecting the virtual temperature correction on CAPE calculations. *Wea. Forecasting,* **9,** 625–629.

——, H. E. Brooks, and R. A. Maddox, 1996: Flash flood forecasting: An ingredients-based methodology. *Wea. Forecasting,* **11,** 560–581.

——, C. Ramis, R. Romero, and S. Alonso, 1998: A diagnostic study of three heavy precipitation episodes in the western Mediterranean region. *Wea. Forecasting,* **13,** 102–124.

Ducrocq, V., 1993: Adiabatic and viscous simulations of symmetric instability: Structure, evolution, and energetics. *J. Atmos. Sci.,* **50,** 23–42.

Dudhia, J., 1993: A nonhydrostatic version of the Penn State–NCAR mesoscale model: Validation tests and simulation of an Atlantic cyclone and cold front. *Mon. Wea. Rev.,* **121,** 1493–1513.

Dunn, L. B., 1988: Vertical motion evaluation of a Colorado snowstorm from a synoptician's perspective. *Wea. Forecasting,* **3,** 261–272.

Eliassen, A., 1990: Transverse circulations in frontal zones. *Extratropical Cyclones, The Erik Palmén Memorial Volume,* C. W. Newton and E. O. Holopainen, Eds., Amer. Meteor. Soc., 155–165.

Emanuel, K. A., 1979: Inertial instability and mesoscale convective systems. Part I: Linear theory of inertial instability in rotating viscous fluids. *J. Atmos. Sci.,* **36,** 2425–2449.

——, 1980: Forced and free mesoscale motions in the atmosphere. *Collection of Lecture Notes on Dynamics of Mesometeorological Disturbances. Proc. CIMMS Symp.* Norman, OK, University of Oklahoma/NOAA, 191–259.

——, 1983a: The Lagrangian parcel dynamics of moist symmetric stability. *J. Atmos. Sci.,* **40,** 2368–2376.

——, 1983b: On assessing local conditional symmetric instability from atmospheric soundings. *Mon. Wea. Rev.,* **111,** 2016–2033.

——, 1983c: Conditional symmetric instability: A theory for rainbands within extratropical cyclones. *Mesoscale Meteorology—Theories, Observations and Models,* D. K. Lilly and T. Gal-Chen, Eds., Reidel, 231–245.

——, 1985: Frontal circulations in the presence of small moist symmetric instability. *J. Atmos. Sci.,* **42,** 1062–1071.

——, 1988: Observational evidence of slantwise convective adjustment. *Mon. Wea. Rev.,* **116,** 1805–1816.

——, 1989: The finite-amplitude nature of tropical cyclogenesis. *J. Atmos. Sci.,* **46,** 3431–3456.

——, 1990: Appendix to chapter 266: Notes on the physical mechanisms of mesoscale precipitation bands. *Radar in Meteorology: Battan Memorial and 40th Anniversary Radar Meteorology Conference,* D. Atlas, Ed., Amer. Meteor. Soc., 473–476.

——, 1992: Slantwise circulations in middle latitude cyclones. Preprints, *Fifth Conf. on Mesoscale Processes,* Atlanta, GA, Amer. Meteor. Soc., 233–234.

——, 1994: *Atmospheric Convection.* Oxford University Press, 580 pp.

Engholm, C. D., E. R. Williams, and R. M. Dole, 1990: Meteorological and electrical conditions associated with positive cloud-to-ground lighting. *Mon. Wea. Rev.,* **118,** 470–487.

Fischer, C., and F. Lalaurette, 1995a: Meso-β-scale circulations in realistic fronts. I: Steady basic state. *Quart. J. Roy. Meteor. Soc.,* **121,** 1255–1283.

——, and ——, 1995b: Meso-β-scale circulations in realistic fronts. II: Frontogenetically forced basic states. *Quart. J. Roy. Meteor. Soc.,* **121,** 1285–1321.

Freedman, J., 1995: Winter season positive cloud-to-ground lightning. M.S. thesis, Dept. of Atmospheric Science, The University at Albany, State University of New York, 121 pp. [Available from Dept. of Earth and Atmospheric Sciences, The University at Albany, State University of New York, Albany, NY 12222.]

Fritsch, J. M., and G. H. Bryan, 1998: Mesoscale convective systems: Slab convective overturning of deep moist absolutely unstable layers. Preprints, *16th Conf. on Weather Analysis and Forecasting,* Phoenix, AZ, Amer. Meteor. Soc., 196–198.

Grumm, R. H., and D. J. Nicosia, 1997: WSR-88D observations of mesoscale precipitation bands over Pennsylvania. *Natl. Wea. Dig.,* **21** (3), 10–23.

Gu, W., Q. Xu, and R. Wu, 1998: Three-dimensional instability of nonlinear viscous symmetric circulations. *J. Atmos. Sci.,* **55,** 3148–3158.

Gyakum, J. R., 1987: Evolution of a surprise snowfall in the United States midwest. *Mon. Wea. Rev.,* **115,** 2322–2345.

Hobbs, P. V., 1978: Organization and structure of clouds and precipitation on the mesoscale and microscale in cyclonic storms. *Rev. Geophys. Space Phys.,* **16,** 741–755.

Hoke, J. E., N. A. Phillips, G. J. DiMego, J. J. Tuccillo, and J. G. Sela, 1989: The Regional Analysis and Forecast System of the National Meteorological Center. *Wea. Forecasting,* **4,** 323–334.

Holle, R. L., and A. I. Watson, 1996: Lightning during two central U.S. winter precipitation events. *Wea. Forecasting,* **11,** 599–614.

Holt, M. W., and A. J. Thorpe, 1991: Localized forcing of slantwise motion at fronts. *Quart. J. Roy. Meteor. Soc.,* **117,** 943–963.

Holton, J. R., 1992: *An Introduction to Dynamic Meteorology.* 3d ed. Academic Press, 511 pp.

Hoskins, B. J., 1974: The role of potential vorticity in symmetric stability and instability. *Quart. J. Roy. Meteor. Soc,* **100,** 480–482.

Houze, R. A., Jr., 1993: *Cloud Dynamics.* Academic Press, 573 pp.

——, 1997: Stratiform precipitation in regions of convection: A meteorological paradox? *Bull. Amer. Meteor. Soc.,* **78,** 2179–2196.

——, S. A. Rutledge, M. I. Biggerstaff, and B. F. Smull, 1989: Interpretation of Doppler weather radar displays of midlatitude mesoscale convective systems. *Bull. Amer. Meteor. Soc.,* **70,** 608–619.

Howard, K., and E. Tollerud, 1988: The structure and evolution of heavy-snow-producing Colorado cyclones. Preprints, *Palmén Memorial Symposium on Extratropical Cyclones,* Helsinki, Finland, Amer. Meteor. Soc., 168–171.

Huo, Z., D.-L. Zhang, J. Gyakum, and A. Staniforth, 1995: A diagnostic analysis of the Superstorm of March 1993. *Mon. Wea. Rev.,* **123,** 1740–1761.

Huschke, R. E., Ed., 1959: *Glossary of Meteorology.* Amer. Meteor. Soc., 638 pp.

Innocentini, V., and E. dos Santos Caetano Neto, 1992: A numerical study of the role of humidity in the updraft driven by moist slantwise convection. *J. Atmos. Sci.,* **49,** 1092–1106.

Jascourt, S. D, S. S. Lindstrom, C. J. Seman, and D. D. Houghton, 1988: An observation of banded convective development in the presence of weak symmetric stability. *Mon. Wea. Rev.,* **116,** 175–191.

Jiang, H., and D. J. Raymond, 1995: Simulation of a mature mesoscale convective system using a nonlinear balance model. *J. Atmos. Sci.,* **52,** 161–175.

Johns, R. H., and C. A. Doswell III, 1992: Severe local storms forecasting. *Wea. Forecasting,* **7,** 588–612.

Jones, S. C., and A. J. Thorpe, 1992: The three-dimensional nature of ''symmetric'' instability. *Quart. J. Roy. Meteor. Soc.,* **118,** 227–258.

Keyser, D., 1999: On the representation and diagnosis of frontal circulations in two and three dimensions. *The Life Cycles of Ex-*

tratropical Cyclones, M. A. Shapiro and S. Grønas, Eds., Amer. Meteor. Soc., 239–264.

——, and L. W. Uccellini, 1987: Regional models: Emerging research tools for synoptic meteorologists. *Bull. Amer. Meteor. Soc.*, **68,** 306–320.

Knight, D. J., and P. V. Hobbs, 1988: The mesoscale and microscale structure and organization of clouds and precipitation in midlatitude cyclones. Part XV: A numerical modeling study of frontogenesis and cold-frontal rainbands. *J. Atmos. Sci.*, **45,** 915–930.

Koch, S. E., D. Hamilton, D. Kramer, and A. Langmaid, 1998: Mesoscale dynamics in the Palm Sunday tornado outbreak. *Mon. Wea. Rev.*, **126,** 2031–2060.

Kristjánsson, J. E., and S. Thorsteinsson, 1995: The structure and evolution of an explosive cyclone near Iceland. *Tellus*, **47A,** 656–670.

Lagouvardos, K., and V. Kotroni, 1995: Upper-level frontogenesis: Two case studies from the FRONTS 87 Experiment. *Mon. Wea. Rev.*, **123,** 1197–1206.

——, Y. Lemaître, and G. Scialom, 1993: Dynamical structure of a wide cold-frontal cloudband observed during FRONTS 87. *Quart. J. Roy. Meteor. Soc.*, **119,** 1291–1319.

Leach, M. J., and J. Kong, 1998: Scale interaction in a California precipitation event. Preprints, *16th Conf. on Weather Analysis and Forecasting*, Phoenix, AZ, Amer. Meteor. Soc., 270–272.

Lemaître, Y., and J. Testud, 1988: Relevance of conditional symmetric instability in the interpretation of wide cold frontal rainbands. A case study: 20 May 1976. *Quart. J. Roy. Meteor. Soc.*, **114,** 259–269.

——, and G. Scialom, 1992: Three-dimensional mesoscale circulation within a convective postfrontal system. Possible role of conditional symmetric instability for triggering convective motion. *Quart. J. Roy. Meteor. Soc.*, **118,** 71–99.

Lilly, D. K., 1986: Instabilities. *Mesoscale Meteorology and Forecasting*, P. S. Ray, Ed., Amer. Meteor. Soc., 259–271.

Lindstrom, S. S., and T. E. Nordeng, 1992: Parameterized slantwise convection in a numerical model. *Mon. Wea. Rev.*, **120,** 742–756.

Locatelli, J. D., J. E. Martin, and P. V. Hobbs, 1994: A wide cold-frontal rainband and its relationship to frontal topography. *Quart. J. Roy. Meteor. Soc.*, **120,** 259–275.

Loughe, A. F., C.-C. Lai, and D. Keyser, 1995: A technique for diagnosing three-dimensional ageostrophic circulations in baroclinic disturbances on limited-area domains. *Mon. Wea. Rev.*, **123,** 1476–1504.

Lussky, G. R., 1989: Heavy rains and flooding in Montana: A case for operational use of symmetric instability diagnosis. *Wea. Forecasting*, **4,** 186–201.

MacGorman, D. R., and W. D. Rust, 1998: *The Electrical Nature of Storms*. Oxford University Press, 422 pp.

Mapes, B. E., 1997: Equilibrium vs. activation control of large-scale variations of tropical deep convection. *The Physics and Parameterization of Moist Atmospheric Convection*, R. K. Smith, Ed., Kluwer, 321–358.

Marécal, V., and Y. Lemaître, 1995: Importance of microphysical processes in the dynamics of a CSI mesoscale frontal cloud band. *Quart. J. Roy. Meteor. Soc.*, **121,** 301–318.

Marks, F. D., Jr., R. A. Houze Jr., and J. F. Gamache, 1992: Dual-aircraft investigation of the inner core of Hurricane Norbert. Part I: Kinematic structure. *J. Atmos. Sci.*, **49,** 919–942.

Martin, J. E., 1998: The structure and evolution of a continental winter cyclone. Part II: Frontal forcing of an extreme snow event. *Mon. Wea. Rev.*, **126,** 329–348.

——, J. D. Locatelli, and P. V. Hobbs, 1992: Organization and structure of clouds and precipitation on the mid-Atlantic coast of the United States. Part V: The role of an upper-level front in the generation of a rainband. *J. Atmos. Sci.*, **49,** 1293–1303.

Mass, C. F., and Y.-H. Kuo, 1998: Regional real-time numerical weather prediction: Current status and future potential. *Bull. Amer. Meteor. Soc.*, **79,** 253–263.

Mathur, M. B., 1983: On the use of lower saturation criteria for release of latent heat in NWP models. *Mon. Wea. Rev.*, **111,** 1882–1885.

——, 1997: Development of an eye-wall like structure in a tropical cyclone model simulation. *Dyn. Atmos. Oceans*, **27,** 527–547.

McCann, D. W., 1995: Three-dimensional computations of equivalent potential vorticity. *Wea. Forecasting*, **10,** 798–802.

——, 1996: Slantwise CAPE—A forecast aid for heavy snow. Preprints, *15th Conf. on Weather Analysis and Forecasting*, Norfolk, VA, Amer. Meteor. Soc., 120–123.

McCarthy, A. K., 1996: Quantitative evaluation of conditional symmetric instability as a mesoscale instability mechanism associated with banded precipitation. M.S. thesis, Dept. of Earth and Atmospheric Sciences, Saint Louis University, 108 pp. [Available from Dept. of Earth and Atmospheric Sciences, Saint Louis University, 3507 Laclede Ave., St. Louis, MO 63103.]

McNulty, R. P., 1978: On upper tropospheric kinematics and severe weather occurrence. *Mon. Wea. Rev.*, **106,** 662–672.

——, 1995: Severe and convective weather: A Central Region forecasting challenge. *Wea. Forecasting*, **10,** 187–202.

Miller, T. L., 1984: The structures and energetics of fully nonlinear symmetric baroclinic waves. *J. Fluid Mech.*, **142,** 343–362.

——, and B. N. Antar, 1986: Viscous nongeostrophic baroclinic instability. *J. Atmos. Sci.*, **43,** 329–338.

Mocko, D. M., and W. R. Cotton, 1995: Evaluation of fractional cloudiness parameterizations for use in a mesoscale model. *J. Atmos. Sci.*, **52,** 2884–2901.

Molinari, J., and M. Dudek, 1992: Parameterization of convective precipitation in mesoscale numerical models: A critical review. *Mon. Wea. Rev.*, **120,** 326–344.

——, P. K. Moore, V. P. Idone, R. W. Henderson, and A. B. Saljoughy, 1994: Cloud-to-ground lightning in Hurricane Andrew. *J. Geophys. Res.*, **99,** 16 665–16 676.

——, P. Moore, and V. Idone, 1999: Convective structure of hurricanes as revealed by lightning locations. *Mon. Wea. Rev.*, **127,** 520–534.

Moore, J. T., and P. D. Blakley, 1988: The role of frontogenetical forcing and conditional symmetric instability in the midwest snowstorm of 30–31 January 1982. *Mon. Wea. Rev.*, **116,** 2155–2171.

——, and T. E. Lambert, 1993: The use of equivalent potential vorticity to diagnose regions of conditional symmetric instability. *Wea. Forecasting*, **8,** 301–308.

Neiman, P. J., M. A. Shapiro, and L. S. Fedor, 1993: The life cycle of an extratropical marine cyclone. Part II: Mesoscale structure and diagnostics. *Mon. Wea. Rev.*, **121,** 2177–2199.

Nordeng, T. E., 1987: The effect of vertical and slantwise convection on the simulation of polar lows. *Tellus*, **39A,** 354–375.

——, 1993: Parameterization of slantwise convection in numerical weather prediction models. *The Representation of Cumulus Convection in Numerical Models, Meteor. Monogr.*, No. 46, Amer. Meteor. Soc., 195–202.

Orville, R. E., R. W. Henderson, and L. F. Bosart, 1988: Bipole patterns revealed by lightning locations in mesoscale storm systems. *Geophys. Res. Lett.*, **15,** 129–132.

Parker, D. J., and A. J. Thorpe, 1995: The role of snow sublimation in frontogenesis. *Quart. J. Roy. Meteor. Soc.*, **121,** 763–782.

Parsons, D. B., and P. V. Hobbs, 1983: The mesoscale and microscale structure and organization of clouds and precipitation in midlatitude cyclones. XI: Comparisons between observational and theoretical aspects of rainbands. *J. Atmos. Sci.*, **40,** 2377–2397.

Persson, P. O. G., 1995: Simulations of the potential vorticity structure and budget of FRONTS 87 IOP8. *Quart. J. Roy. Meteor. Soc.*, **121,** 1041–1081.

——, and T. T. Warner, 1991: Model generation of spurious gravity waves due to inconsistency of the vertical and horizontal resolution. *Mon. Wea. Rev.*, **119,** 917–935.

——, and ——, 1993: Nonlinear hydrostatic conditional symmetric instability: Implications for numerical weather prediction. *Mon. Wea. Rev.*, **121,** 1821–1833.

——, and ——, 1995: The nonlinear evolution of idealized, unforced, conditional symmetric instability: A numerical study. *J. Atmos. Sci.*, **52,** 3449–3474.

Ramstrom, W. D., 1990: Wind patterns in New England coastal

storms. B.S. thesis, Dept. of Electrical Engineering and Computer Science, Massachusetts Institute of Technology, 32 pp. [Available from Dept. of Electrical Engineering and Computer Science, M.I.T., 77 Massachusetts Ave., Cambridge, MA 02139.]

Rauber, R. M., M. K. Ramamurthy, and A. Tokay, 1994: Synoptic and mesoscale structure of a severe freezing rain event: The St. Valentine's Day ice storm. *Wea. Forecasting,* **9,** 183–208.

Reuter, G. W., and M. K. Yau, 1990: Observations of slantwise convective instability in winter cyclones. *Mon. Wea. Rev.,* **118,** 447–458.

——, and N. Aktary, 1993: A slantwise Showalter index based on moist symmetric instability: Results for central Alberta. *Atmos.–Ocean,* **31,** 379–394.

——, and C. D. Nguyen, 1993: Organization of cloud and precipitation in an Alberta storm. *Atmos. Res.,* **30,** 127–141.

——, and M. K. Yau, 1993: Assessment of slantwise convection in ERICA cyclones. *Mon. Wea. Rev.,* **121,** 375–386.

——, and N. Aktary, 1995: Convective and symmetric instabilities and their effects on precipitation: Seasonal variations in central Alberta during 1990 and 1991. *Mon. Wea. Rev.,* **123,** 153–162.

——, and R. Beaubien, 1996: Radar observations of snow formation in a warm pre-frontal snowband. *Atmos.–Ocean,* **34,** 605–626.

Rivas Soriano, L. J., and E. L. García Díez, 1997: Effect of ice on the generation of a generalized potential vorticity. *J. Atmos. Sci.,* **54,** 1385–1387.

Rogers, R. R., and M. K. Yau, 1989: *A Short Course in Cloud Physics.* 3d ed. Pergamon Press, 293 pp.

Saitoh, S., and H. Tanaka, 1987: Numerical experiments of conditional symmetric baroclinic instability as a possible cause for frontal rainband formation Part I. A basic experiment. *J. Meteor. Soc. Japan,* **65,** 675–708.

——, and ——, 1988: Numerical experiments of conditional symmetric baroclinic instability as a possible cause for frontal rainband formation Part II. Effects of water vapor supply. *J. Meteor. Soc. Japan,* **66,** 39–53.

Sanders, F., 1986: Frontogenesis and symmetric stability in a major New England snowstorm. *Mon. Wea. Rev.,* **114,** 1847–1862.

——, and L. F. Bosart, 1985: Mesoscale structure in the Megalopolitan snowstorm of 11–12 February 1983. Part I: Frontogenetical forcing and symmetric instability. *J. Atmos. Sci.,* **42,** 1050–1061.

Seltzer, M. A., R. E. Passarelli, and K. A. Emanuel, 1985: The possible role of symmetric instability in the formation of precipitation bands. *J. Atmos. Sci.,* **42,** 2207–2219.

Seman, C. J., 1991: Numerical study of nonlinear convective–symmetric instability in a rotating baroclinic atmosphere. Ph.D. dissertation, 185 pp. [Available from University of Wisconsin—Madison, Dept. of Atmospheric and Oceanic Sciences, Madison, WI 53706.]

——, 1992: On the role of nonlinear convective–symmetric instability in the evolution of a numerically simulated mesoscale convective system. Preprints, *Fifth Conf. on Mesoscale Processes,* Atlanta, GA, Amer. Meteor. Soc., 282–287.

——, 1994: A numerical study of nonlinear nonhydrostatic conditional symmetric instability in a convectively unstable atmosphere. *J. Atmos. Sci.,* **51,** 1352–1371.

Shields, M. T., R. M. Rauber, and M. K. Ramamurthy, 1991: Dynamical forcing and mesoscale organization of precipitation bands in a midwest winter cyclonic storm. *Mon. Wea. Rev.,* **119,** 936–964.

Shutts, G. J., 1990: SCAPE charts from numerical weather prediction model fields. *Mon. Wea. Rev.,* **118,** 2745–2751.

——, and M. J. P. Cullen, 1987: Parcel stability and its relation to semigeostrophic theory. *J. Atmos. Sci.,* **44,** 1318–1330.

Snook, J. S., 1992: Current techniques for real-time evaluation of conditional symmetric instability. *Wea. Forecasting,* **7,** 430–439.

Stensrud, D. J., R. A. Maddox, and C. L. Ziegler, 1991: A sublimation-initiated mesoscale downdraft and its relation to the wind field below a precipitating anvil cloud. *Mon. Wea. Rev.,* **119,** 2124–2139.

Thorpe, A. J., and K. A. Emanuel, 1985: Frontogenesis in the presence of small stability to slantwise convection. *J. Atmos. Sci.,* **42,** 1809–1824.

——, and R. Rotunno, 1989: Nonlinear aspects of symmetric instability. *J. Atmos. Sci.,* **46,** 1285–1299.

——, and S. A. Clough, 1991: Mesoscale dynamics of cold fronts: Structures described by dropsoundings in FRONTS 87. *Quart. J. Roy. Meteor. Soc.,* **117,** 903–941.

——, B. J. Hoskins, and V. Innocentini, 1989: The parcel method in a baroclinic atmosphere. *J. Atmos. Sci.,* **46,** 1274–1284.

van Mieghem, J. M., 1951: Hydrodynamic instability. *Compendium of Meteorology,* T. F. Malone, Ed., Amer. Meteor. Soc., 434–453.

Vonnegut, B., 1994: The atmospheric electricity paradigm. *Bull. Amer. Meteor. Soc.,* **75,** 53–61.

Wallace, J. M., and P. V. Hobbs, 1977: *Atmospheric Science: An Introductory Survey.* Academic Press, 467 pp.

Wang, P., Z. Xu, and Z. Pan, 1990: A case study of warm sector rainbands in north China. *Adv. Atmos. Sci.,* **7,** 354–365.

Weisman, R. A., 1996: The Fargo snowstorm of 6–8 January 1989. *Wea. Forecasting,* **11,** 198–215.

Wiesmueller, J. L., and S. M. Zubrick, 1998: Evaluation and application of conditional symmetric instability, equivalent potential vorticity, and frontogenetical forcing in an operational forecasting environment. *Wea. Forecasting,* **13,** 84–101.

Williams, E., 1991: Comments on ''Thunderstorms above frontal surfaces in environments without positive CAPE. Part I: A climatology.'' *Mon. Wea. Rev.,* **119,** 2511–2513.

——, and N. Renno, 1993: An analysis of the conditional instability of the tropical atmosphere. *Mon. Wea. Rev.,* **121,** 21–36.

Wolfsberg, D. G., K. A. Emanuel, and R. E. Passarelli, 1986: Band formation in a New England winter storm. *Mon. Wea. Rev.,* **114,** 1552–1569.

Wood, L. T., and J. W. Nielsen-Gammon, 1994: Synthetic dual-Doppler analysis of a wintertime rainband. Preprints, *Sixth Conf. on Mesoscale Processes.* Portland, OR, Amer. Meteor. Soc., 640–643.

Xu, K.-M., and K. A. Emanuel, 1989: Is the tropical atmosphere conditionally unstable? *Mon. Wea. Rev.,* **117,** 1471–1479.

Xu, Q., 1986a: Conditional symmetric instability and mesoscale rainbands. *Quart. J. Roy. Meteor. Soc.,* **112,** 315–334.

——, 1986b: Generalized energetics for linear and nonlinear symmetric instabilities. *J. Atmos. Sci.,* **43,** 972–984.

——, 1989a: Extended Sawyer–Eliassen equation for frontal circulations in the presence of small viscous moist symmetric stability. *J. Atmos. Sci.,* **46,** 2671–2683.

——, 1989b: Frontal circulations in the presence of small viscous moist symmetric stability and weak forcing. *Quart. J. Roy. Meteor. Soc.,* **115,** 1325–1353.

——, 1992: Formation and evolution of frontal rainbands and geostrophic potential vorticity anomalies. *J. Atmos. Sci.,* **49,** 629–648.

——, 1994: Semibalance model—Connection between geostrophic-type and balanced-type intermediate models. *J. Atmos. Sci.,* **51,** 953–970.

——, and J. H. E. Clark, 1985: The nature of symmetric instability and its similarity to convective and inertial instability. *J. Atmos. Sci.,* **42,** 2880–2883.

Zhang, D.-L., and H.-R. Cho, 1992: The development of negative moist potential vorticity in the stratiform region of a simulated squall line. *Mon. Wea. Rev.,* **120,** 1322–1341.

——, and ——, 1995: Three-dimensional simulation of frontal rainbands and conditional symmetric instability in the Eady-wave model. *Tellus,* **47A,** 45–61.

Zhao, Q., T. L. Black, and M. E. Baldwin, 1997: Implementation of the cloud prediction scheme in the Eta model at NCEP. *Wea. Forecasting,* **12,** 697–712.

Ziegler, C. L., and E. N. Rasmussen, 1998: The initiation of moist convection at the dryline: Forecasting issues from a case study perspective. *Wea. Forecasting,* **13,** 1106–1131.

CORRIGENDUM

Due to a production error in ''The Use and Misuse of Conditional Symmetric Instability,'' by David M. Schultz and Philip N. Schumacher, *Monthly Weather Review*, Vol. 127, No. 12, 2709–2732, one of the figures appeared incorrectly.

The correct Fig. 5a appears below.

The staff of the *Monthly Weather Review* regrets any confusion this error may have caused.

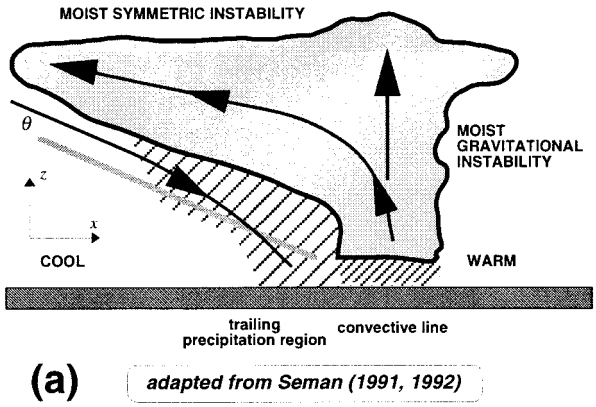

FIG. 5a. Schematic cross section of upscale convective–symmetric instability in a midlatitude mesoscale convective system [adapted from Seman (1991, 1992)]. Thick solid line encloses cloud (shaded). Thin solid lines with arrows represents direction of circulation. Gray solid line labeled represents orientation of typical potential-temperature contour in the cool air. Hatching is proportional to precipitation intensity. Moist gravitational instability is released within the convective line, remaining moist symmetric instability is released within the trailing precipitation region; dry-adiabatic descent initially occurs within rear inflow, which may become saturated due to precipitation evaporating/sublimating into the descending air.